

Multi-Sensor Calibration of an Integrated Mobile Mapping Platform

Undergraduate Honors Thesis

Presented in Partial Fulfillment of the Requirements for  
Graduation with Distinction  
at The Ohio State University

By

Justin Luvene Crawford

Undergraduate Program in Geomatics Engineering.

The Ohio State University

2012

Thesis Committee:

Dr. Dorota Grejner-Brzezinska, Advisor

Dr. Alper Yilmaz

Copyright by  
Justin Luvene Crawford  
2012

## Abstract

A Mobile Mapping System can be defined as a kinematic platform, upon which multiple sensors have been integrated and synchronized to a common time base, to provide three-dimensional near-continuous and automatic positioning of both the platform and simultaneously collected geo-spatial data [Grejner-Brzezinska, 2001a]. These systems are composed of three principle types of sensors: Global Positioning System (GPS) receivers, an Inertial Navigation System (INS), and imaging sensors (cameras/LIDAR) (Light Detection and Ranging). Left alone, the sensors would all record independent measurements in separate reference frames that would be of no use for real-time mapping. Hence the need for a multi-sensor calibration, defined here as the process of determining the translational and rotational offsets between the sensors, to bring all sensor data into the same reference frame.

The inter-relationships among the sensors will be determined in two steps through the use of contemporary surveying and photogrammetric techniques. First, the position of all sensors will be precisely surveyed to determine with high accuracy the position of the sensor where data is recorded. Since the positions of these sensors are measured in the same coordinate system, they can be related to a common sensor, the INS in this case, through translation and rotation with respect to the data recording point of the INS and the INS body axes. Secondly, photogrammetric techniques will be applied to determine the translational offsets needed to relate the surveyed center of each camera to the camera

perspective center and the rotational offsets needed to relate the camera frame to the INS body frame. Additionally, the relative orientation will be computed for each pair of stereo cameras (front and back) to determine the translational and rotational offsets between them, allowing for the creation of a stereo model by the extraction of three-dimensional information from the overlapping fields of view of these cameras.

In determining sensor inter-relationships it is important to retain a high accuracy standard on the survey, as all relationships are determined based on the initial survey results of the sensors and ground control points. Failure to maintain a high accuracy will directly result in an incorrect alignment and orientation between sensors. This, in turn, can result in the extraction of incorrect geo-spatial information from the imagery and the extraction of incorrect navigation information if image-to-image matching is used for navigation. It is, therefore, important to ensure that the highest level of accuracy is obtained, which is accomplished through choosing an appropriate level of precision, following good surveying practices, and performing checks on measurements to detect and remove errors.

Dedicated to my family.

## Acknowledgments

I would like to thank my advisor, Dr. Dorota Grejner-Brzezinska, for exposing me to research on multi-sensor calibration. I am thankful for her invaluable guidance, encouragement, and advice throughout my research.

I am grateful to Dr. Charles Toth for his constant support and technical guidance.

I would like to thank my fellow students at The Ohio State University SPIN Lab for help with data processing.

## Vita

June 2006 ..... Eastmoor Academy High School

2010 to 2012..... Undergraduate Research Assistant, Mapping  
and GIS Lab, The Ohio State University

2012 to present ..... Undergraduate Research Assistant, SPIN  
Lab, The Ohio State University

2012..... B.S. Geomatics Engineering, The Ohio State  
University

## Fields of Study

Major Field: Geomatics Engineering.

## Table of Contents

Multi-Sensor Calibration of an Integrated Mobile Mapping Platform.....	1
Undergraduate Honors Thesis.....	1
Abstract.....	ii
Dedicated to my family.....	iv
Acknowledgments .....	v
Vita .....	vi
Fields of Study .....	vi
Table of Contents .....	vii
List of Tables.....	x
List of Figures .....	xi
Chapter 1 Introduction.....	1
1.1 Introduction.....	1
1.2 GPSVan Sensors .....	5
1.2.1 Inertial Navigation System.....	5
1.2.2 NAVSTAR Global Positioning System.....	6



1.2.3 Digital Cameras .....	7
1.3 Earth Models.....	10
1.3.1 Introduction .....	10
1.3.2 Reference Surfaces .....	11
1.3.3 Earth Surfaces.....	13
1.4 Common Reference Frames .....	16
1.4.1 The Earth Centered Earth Fixed (ECEF) Frame .....	16
1.4.2 The Navigation Frame .....	17
1.4.3 The Mapping Frame.....	17
1.4.4 The Body Frame .....	18
1.4.5 Photo Coordinate System.....	20
1.4.6 Image Coordinate System .....	21
1.5 Overview .....	22
Chapter 2 Lever Arm Determination.....	24
2.1 Introduction.....	24
2.2 Sensor Survey .....	25
2.2.1 GPSVan Survey .....	27
2.2.2 Ground Control Point Survey .....	39
2.3 Lever Arm Computation.....	46

Chapter 3 Camera Inter-relationships .....	50
3.1 Introduction.....	50
3.2 Boresight Transformation.....	51
3.2.1 Introduction .....	51
3.2.2 Correcting Camera Lens Distortion.....	52
3.2.3 Image Resection .....	55
3.2.4 Computation of INS and Camera Lever Arms .....	62
3.2.5 Determination of the Boresight Matrix .....	63
3.3 Relative Orientation .....	65
3.3.1 Introduction .....	65
3.3.2 Computing Relative Orientation.....	67
Chapter 4 Conclusions and Future Work.....	70
References .....	73

## List of Tables

Table 2.1: GPSVan Sensor Identification.....	31
Table 2.2: Sensor Lever Arm Components.....	49
Table 3.1: Resection Results .....	69
Table 3.2: Relative Orientation Results .....	69

## List of Figures

Figure 1.1: The Sensor Network Outside of the GPSVan .....	4
Figure 1.2: The Multiple INS Sensors Inside the GPSVan Outlined in Blue. ....	5
Figure 1.3: Direct Georeferencing.....	10
Figure 1.4: Elements of an Ellipsoid of Revolution .....	13
Figure 1.5: Earth Surface Relationships .....	15
Figure 1.6: The ECEF Frame and the Navigation Frame .....	18
Figure 1.7: Body Frame Definition .....	19
Figure 1.8: Body Frame Rotations .....	20
Figure 1.9: The Photo Coordinate System.....	21
Figure 1.10: Image Coordinate System .....	22
Figure 2.1: Leica TS02 Total Station .....	26
Figure 2.2: Fiducial Mark from Control Network.....	28
Figure 2.3: Entire Fiducial Mark Control Network Inside Center for Automotive Research. ....	28
Figure 2.4: Visual Representation of the Fiducial Control Network.....	29
Figure 2.5: Setup Locations Relative to GPSVan. ....	30
Figure 2.6: Distance and Zenith Angle Determination.....	32
Figure 2.7: Northing and Easting Determination .....	33

Figure 2.8: Main Antenna Survey Points.....	35
Figure 2.9: INS Survey Points .....	38
Figure 2.10: Camera Survey Points.....	39
Figure 2.11: Exterior Ground Control Points.....	41
Figure 2.12: Driver's Side View of Lever Arm Components. ....	48
Figure 2.13: Rear View of Lever Arm Components. ....	49
Figure 3.1: Camera Resection .....	56
Figure 3.2: Left Front Stereo Camera Images.....	58
Figure 3.3: Dependent Relative Orientation Geometry .....	67

## Chapter 1 Introduction

### 1.1 Introduction

Over the past couple decades mobile mapping systems have developed from simple land-based systems to complex multi-sensor systems capable of producing real-time solutions in land and airborne environments. The growth of mobile mapping technology is particularly noticeable in remote sensing, surveying, and mapping, where such systems are not only used to keep track of the platform (satellite, airplane, or in this case, van), but are used to affix a spatial reference to data at the three-dimensional coordinates where it was acquired. This adds a temporal component to analysis, as data is able to be recorded from the same area on a repeatable basis, allowing for the monitoring of such things as urban growth, vegetation coverage, crop growth cycles, and erosion to name only a few. However, the sensors must first be calibrated and integrated into a consistent data frame before such a spatial connection can be made.

System calibration first requires that the positions of all sensors are precisely surveyed in a common reference frame, referred here after as the body frame. Next, the image coordinates obtained from stereoscopic images must be transformed into the mapping frame. The transformation between the image coordinates specified in the camera frame and the selected mapping reference frame is called image georeferencing or

sensor orientation [Skaloud et al., 1996]. After the georeferencing, the images are properly oriented and stitched together, the image coordinates are transformed from relative to absolute, and are now tied to a geodetic datum (referred to earlier as common mapping reference frame). In modern mapping, image georeferencing is provided by an integrated system based on the Global Positioning System (GPS) and inertial navigation system (INS). GPS and INS are complementary systems, and they form a reliable image georeferencing system. The INS is a relative positioning system providing direct accelerations and angular rates measured by accelerometers and gyroscopes as a function of time. Once inertial error compensations have been applied, these observations are used to predict future navigation parameters, which will be used in the linearization of the GPS measurements. The GPS observations are applied as measurement updates to correct the predicted position, velocity, and attitude parameters of the INS, as well as to estimate errors in the inertial sensors, that is accelerometers and gyroscopes. GPS, unlike INS, provides position and velocity observations with a high absolute accuracy. While INS observations are made as a function of time, unlike GPS, they lack stability over time since inertial sensor errors grow in time and require calibration by independent absolute positioning sensors, such as GPS. To this end GPS is used wherever possible to estimate the inertial sensor errors in order to correct the INS observations that can be used to predict high accuracy navigation parameters over short-term obstructions in GPS coverage (overpasses, tunnels, heavy vegetation, and urban canyons).

The sensors to be used in this multi-sensor calibration are the GPS antennas, the INS, and the digital cameras. Figure 1.1 shows the location of the sensors on top of the

GPSVan, which represents a mobile mapping system. The location of the GPS antennas and the camera positions are outlined in red and pink rectangles, respectively. Note that the GPS antenna from the rightmost location is not seen in the image as it is being fitted with an extender to increase its height with respect to the surrounding sensors and improve the quality of signal reception from GPS satellites. Also, there are four additional cameras hidden in this view: two in the front and two additional cameras, whose location is a mirror of the two visible cameras. The two cameras positioned on the sides of the GPSVan are mono cameras, meaning they offer a single field of view. The two cameras in the front and two cameras in the back form two sets of stereo cameras. Stereo cameras consist of a pair of cameras that are placed a set distance apart and oriented in a similar direction so that their fields of view overlap. Each camera has a different perspective of the overlapping area, which can be used to generate a stereo model to abstract three-dimensional coordinates of features in the overlapping field of view. Creating a stereo model will require additional knowledge about the position and orientation of the cameras with respect to each other, which will be determined during sensor calibration. Figure 1.2 shows the components of the INS outlined in blue; note that INS is mounted inside the vehicle, as this system does not require any line-of-sight to collect navigation information. A brief explanation of each sensor and the associated calibration procedure follows.





Figure 1.1: The Sensor Network Outside of the GPSVan. The red rectangles outline the position of the GPS antennas and the pink rectangles outline the two cameras visible in this view of the GPSVan.



Figure 1.2: The Multiple INS Sensors Inside the GPSVan Outlined in Blue.

The rest of this chapter will introduce terms, concepts, and definitions needed in the following chapters.

## 1.2 GPSVan Sensors

### *1.2.1 Inertial Navigation System*

An inertial navigation system comprises a set of six inertial measurement units (IMUs)-three accelerometers and three gyroscopes, the platform on which they are mounted (including the stabilization mechanism, if so provided) and the computer that performs the calculations needed to transform sensed accelerations and, in some

mechanizations, the angles or angular rates into navigationally useful information: position, velocity, and attitude [Jekeli, 2001]. The INS is used to obtain navigation information (three position coordinates, three velocity components, and three attitude angles) in place of the GPS in areas where the GPS signal is obstructed, such as under bridges, in tunnels, under trees, and between GPS measurement updates. Note that the sampling rate of the INS is up to four hundred Hertz, while the sampling rate of the surveying grade GPS receivers is, generally, up to twenty hertz. However, the long-term accuracy of a stand-alone INS is poor in comparison to GPS and a high accuracy navigation solution cannot be provided over a long period of time. These two sensors work together to provide a continuous and accurate navigation/georeferencing solution. Since the GPS antenna and INS are physically separated in the mobile mapping platform, the transformation parameters (or linear offsets that are also referred to as lever arm offsets) that define the location of the GPS antenna phase center with respect to the INS body frame must be determined, once the sensors are mounted in the vehicle. Sensor calibration, which results in determination of the transformation between INS and GPS, requires precise surveying of GPS antenna phase center location, with respect to an INS body frame.

### *1.2.2 NAVSTAR Global Positioning System*

The NAVSTAR Global Positioning System is a satellite-based radio-positioning and time-transfer system, designed, financed, deployed, and operated by the US Department of Defense (DoD). It was designed as an all-weather, continuous, global radio-navigation system [Wooden, 1985]. GPS receivers need to receive a signal from a

minimum of four satellites simultaneously in order to correct the clock offset between the satellite and the receiver and solve for a unique XYZ position defined in a global geodetic datum called WGS84. These measurements are made to the phase center of the antenna, which would be the ideal point to survey for calibration. However, the phase center is located inside the antenna and can be found with respect to the base plane of the antenna according to specifications provided by the manufacturer. The GPS calibration component is focused on measuring the GPS/INS lever arm, or the offset of the receiver phase center from the INS body frame (defined by the manufacturer). Calibration of the GPS/INS lever arm offsets can be accomplished through a precise survey to determine the coordinates of the GPS antenna reference points, in the INS body frame. Since both GPS and INS navigate in the same reference system (WGS84), a precise survey performed in this reference system (referred to as a mapping frame here) allows for direct estimation of linear offsets between the two sensors.

### *1.2.3 Digital Cameras*

In all-digital mobile mapping, the camera georegistration (also referred to as exterior orientation parameters) are determined directly by GPS/INS. The exterior orientation parameters define the position and the orientation of the camera at the moment of exposure. For a mapping system to function properly, cameras must be calibrated, and an inter-calibration between the cameras and GPS/INS must be determined. The camera calibration/inter-calibration consists of two parts: determination of the interior orientation parameters and derivation of the boresight transformation (three linear offsets and three orientation parameters) between the camera frame and the INS

body frame). The exterior orientation parameters directly define the position and the orientation of the camera at the moment of exposure. These are determined through precise surveying in a common reference frame and related to the INS body frame by translational and rotational offsets. The interior orientation parameters are concerned with modeling the camera projection system and determination of the principal point coordinates, focal length, and lens geometric distortion characteristics. The principle point is mathematically defined as the foot of the perpendicular dropped from the perspective center to the plane of the photograph and is illustrated in Figure 1.9. The perspective center is the center through which all points are projected onto the reference plane. The positions and orientations from the GPS/INS do not refer to the perspective center of the imaging sensor directly [Grejner-Brzezinska and Toth, 2000]. Consequently, as already explained, camera calibration requires an additional step, the boresight transformation. Boresighting is the process of deriving a transformation between the camera reference frame and the INS reference frame. This transformation consists of two parts: computation of the displacement between the center of the INS body frame and the camera projection center as well as the determination of the rotation matrix between the INS body frame and the camera optical axis.

After the camera calibration, when the relationship between the camera perspective center and the INS body frame is known, object points in the mapping frame can be directly georeferenced. This georeferencing is done through the direct georeferencing equation [Grejner-Brzezinska. 2012], utilizing the camera and INS inter-relationships depicted in Figure 1.3. The direct georeferencing equation is given as:

$$r_{M,k} = r_{M,INS} + R_{BINS}^M (s \times R_C^{BINS} \times r_{m,i,j} + b_{BINS}) \quad (1.1)$$

Where

$r_{M,k}$  is the vector of three-dimensional coordinates of a point (object) in the mapping frame, represented as the large circle in Figure 1.3

$r_{M,INS}$  is the vector of three-dimensional coordinates of the INS in the mapping frame measured by GPS/INS

$R_{BINS}^M$  is the rotation matrix between the INS body frame and mapping frame (M) measured by the INS

$s$  is a scaling factor

$R_C^{BINS}$  is the boresight rotation matrix between the INS body frame and camera frame (or stereo-model frame)

$r_{m,i,j}$  is the vector of three-dimensional object coordinates in the model frame (derived from the i,j stereo pair attached to the camera frame)

$b_{BINS}$  is the vector of three linear boresight offset components of the camera in the INS body frame

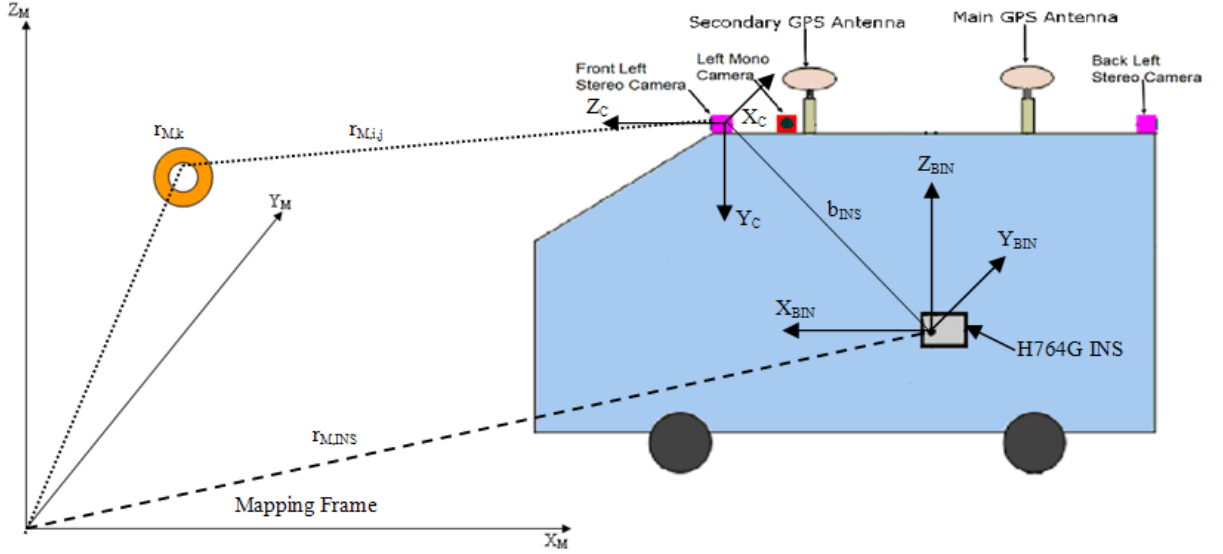


Figure 1.3: Direct Georeferencing. This figure illustrates the process of georeferencing of a point (object) on the ground (yellow circle) using the direct georeferencing equation. It is assumed that the system has already been calibrated, so that the position of the GPS antenna phase center (lever arm vector) and the boresight matrix and linear offsets of the camera are known in the INS body frame. The vector of three-dimensional coordinates of the INS in the mapping frame (M) is denoted by the dashed line with the long dashes (corresponds to vector  $r_{M,INS}$  in eq. (1.1)). The solid line between the camera and INS denotes the boresight vector,  $b_{INS}$ , between the INS and camera, the dotted line from the camera to the yellow circle represents the three-dimensional vector of coordinates of an object (point),  $r_{m,i,j}$ , in the camera (or stereo-model) frame, and the dotted line from the yellow circle to the origin of the mapping frame is the three-dimensional vector,  $r_{M,k}$  in eq. (1.1) of the object (point) in the mapping frame.

## 1.3 Earth Models

### 1.3.1 Introduction

The shape and surface of the earth are complicated to model, but they must be accurately modeled in order to determine the position of a point on the earth. Geodetic datums or reference systems have been specifically defined to handle this task. A geodetic datum defines the shape, size position, and orientation of a (mathematical)

reference surface (e.g. sphere or ellipsoid) [Grejner-Brzezinska, 2011]. Hundreds of datums have been defined and vary in terms of the reference surface used and the origin of the reference surface with respect to what they are created to model. Contemporary geodetic datums range from flat-earth models used for plane surveying to complex models used for international applications, which completely describe the size, shape, orientation, gravity field, and angular velocity of the earth. Additionally, the mathematical reference surface of a geodetic datum can be defined on a local or global basis. A global reference surface is an ellipsoid created with its origin at a set point so that it can serve as a best fit to the entire earth. Local datums use a variety of reference surfaces with an origin positioned to best represent a specific geographically defined region of the earth.

### *1.3.2 Reference Surfaces*

As mentioned above, there are a variety of available reference surfaces, each created depending on the application of the geodetic datum. Reference surfaces are mathematical models of the earth's surface used to describe the position of a point. These models range from flat-earth models to spherical models, and more complex ellipsoidal models derived from years of satellite measurements. Additionally, the choice of a particular reference surface depends on the accuracy and scale of an application. For example, an ellipsoidal reference surface would be used to describe geographic positions for surveying, mapping, and navigation on a worldwide basis. Conversely, a local area survey may choose a flat-earth model by projecting the complex surface of the earth onto



a two-dimensional grid surface. Some of the more commonly used models are explained below:

- Flat Earth Models—Flat earth models are still used for plane surveying over distances short enough so that the earth curvature is insignificant. These are generally distance less than ten kilometers. Over larger area plane surveying projects, multiple flat-earth models can be defined to increase the accuracy over the project area through better approximating the true projective shape of the earth by reducing the size of each model area, thus reducing the effects of projective distortion caused by the Earth's curvature.
- Spherical Earth Models—Spherical earth models represent the shape of the earth with a sphere of a specified radius. Spherical earth models are often used for short range navigation and for global distance approximations. Spherical models fail to model the actual shape of the earth caused by the slight flattening of the earth at the poles results in about a twenty kilometer difference at the poles between an average spherical radius and the measured polar radius of the earth [Grejner-Brzezinska, 2011]. These models are commonly used in the most basic, elementary descriptions of the Earth.
- Ellipsoidal Earth Models—Ellipsoidal earth models are required for precise distance and direction measurement over long distances [Ramirez, 2010]. An ellipsoid is a mathematic figure generated by rotating an ellipse around its polar or minor axis. These models account for the slight flattening of the earth at the poles and serve as a better representation of the shape of the earth than spherical

earth models. While these models do allow for accurate distance and direction measurement they are not able to provide an accurate height. The best global ellipsoidal models can represent the shape of the over the smoothed, averaged sea-surface to within about one-hundred meters [Ramirez, 2010]. The elements of a typical ellipsoid of revolution are shown in Figure 1.4 below.

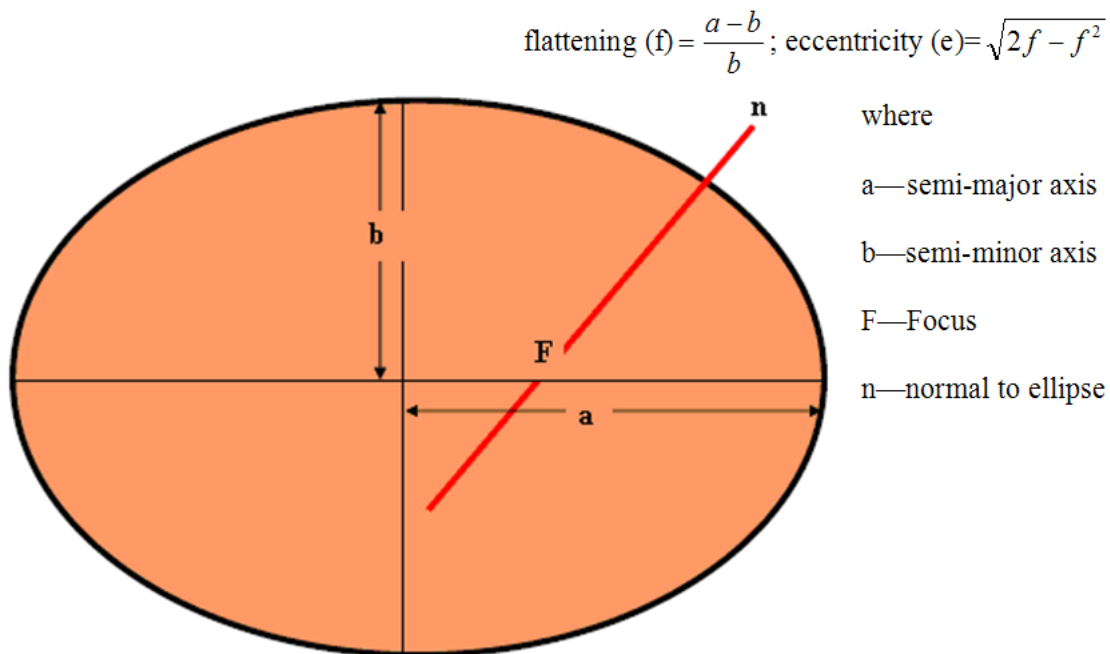


Figure 1.4: Elements of an Ellipsoid of Revolution

### 1.3.3 Earth Surfaces

The actual earth surface is highly irregular and constantly changing. Consequently, it cannot be accurately modeled mathematically, but must be empirically modeled. Some of the most common earth surfaces used in navigation, surveying, and mapping are discussed below:

- **Topographic Surface**—The actual surface of the land and sea at some moment in time [Ramirez, 2010]. Aircraft navigators have a special interest in maintaining a positive height vector above this surface.
- **Sea Level**—Sea level can be thought of as the average surface of the oceans [Ramirez, 2010]. This surface is quite complicated, as tidal forces and gravity differences vary by location and can cause the smoothed sea level surface to vary by hundreds of meters across the globe. The concept of a sea level surface is most commonly used in orthometric height determination through spirit leveling, where the mean sea level serves as the zero basis from which all heights are measured. The mean sea level is determined as the hourly water elevations observed over a 19-year cycle. This period of observations takes into account the variations in tidal highs and lows caused by the changing effects of the gravitational forces from the moon and sun.
- **Geoid Models**—The geoid is an equipotential surface of the Earth's gravity field which would coincide with the ocean surface if the latter were undisturbed and affected only by the Earth's gravity field [Ho, 2009]. These are physical models with no mathematical expression representing the entire earth as a continuous surface, very similar to the mean sea level surface, and extending under continents. The geoid surface is the true zero surface for measuring orthometric heights. The geoid height,  $N$  (also referred to as geoid undulation), can be related to the ellipsoidal,  $h$ , and orthometric,  $H$ , heights as:

$$h=H+N \quad (1.2)$$

Where

$h$ —ellipsoidal height

$H$ —orthometric height

$N$ —geoid height (undulation) provided, for example, by the USGG2009 geoid model <<http://www.ngs.noaa.gov/GEOID/USGG2009/>>.

Rearranging equation 1.2 to solve for the geoid height yields:

$$N=h-H \quad (1.3)$$

The relationship between orthometric heights, geoid heights and ellipsoid heights is shown in Figure 1.5. In Figure 1.5 the deflection of the vertical ( $\theta$ ), which is the angle between the normal to the ellipsoid and the normal to the geoid and or vertical line calculated by a plumb bob as the perpendicular to gravity at that point.

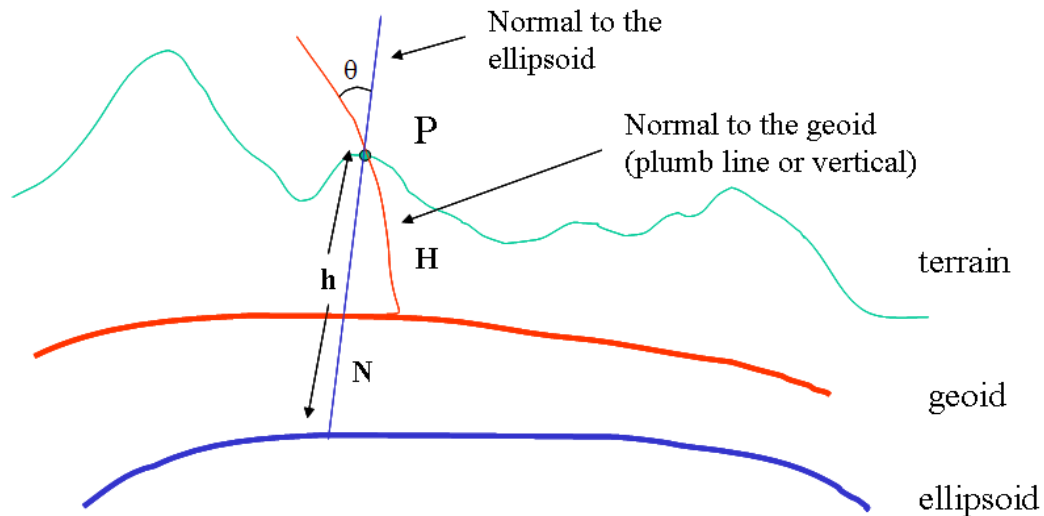


Figure 1.5: Earth Surface Relationships. Elevation of point P on the Earth's surface as described by the height above the ellipsoid ( $h$ ), the height above the geoid ( $H$ ) and the geoid undulation ( $N$ ) or the separation between the ellipsoid and geoid used to relate the two heights. Also shown is  $\theta$ , the deflection of the vertical. This is the angle made between the curve normal to the ellipsoid and the curve normal to the geoid.

## 1.4 Common Reference Frames

Relating the reference frames between the different sensors is the core function of multi-sensor calibration. To this end, some of the major reference systems will be discussed.

### *1.4.1 The Earth Centered Earth Fixed (ECEF) Frame*

The ECEF frame has its origin at the center of mass of the earth and its axes are fixed with respect to the earth (the frame rotates with the earth). The XY plane of this system coincides with the equatorial plane, so that the x-axis points to the Greenwich (prime) meridian and designates the zeros from which angles are turned. The positive y-axis is defined to point in the direction ninety degrees counter-clockwise of the positive x-axis, and the z-axis is oriented so that it is parallel to the Earth's mean spin axis. The main advantage of this system is that locations of all points are measured from the center of mass of the earth and refer to the same triad of geocentric axes. Coordinates of a point in ECEF frame can be represented as three dimensional Cartesian coordinates as well as geodetic coordinates, and there exist simple transformations between them for given parameters of a reference ellipsoid. Geodetic coordinates describe a point in terms of latitude, longitude, and height, where longitude is the angle turned from the positive x-axis, latitude is the angle turned from the equatorial plane, and height is the height above the ellipsoid. Figure 1.6 shows the representation of a point in the ECEF frame and the ability to express it as either Cartesian (X, Y, Z) or geodetic ( $\lambda$ ,  $\phi$ , h) coordinates.

#### *1.4.2 The Navigation Frame*

The navigation frame is a local geodetic frame, which has its origin coinciding with that of the sensor frame (in the application described here), and its axes form a north-east-down (NED) system or an east-north-up (ENU) system. The NED system is defined so that the x-axis of the sensor points towards geodetic north, the z-axis is orthogonal to the reference ellipsoid with the positive direction pointing down, and the positive y-axis points in the east direction. The major advantages of this system are that the direction of a right turn is in the positive direction with respect to a downward axis and the axes coincide with vehicle-fixed roll, pitch, and heading coordinates when the vehicle is level and headed North. In the ENU system, the positive x-axis points in the east direction, the positive y-axis points in the north direction, and the positive z-axis points in the up direction. The major advantage of this frame is that altitude increases in the upward direction.

#### *1.4.3 The Mapping Frame*

The mapping frame is a reference frame where the final mapping product will be delivered. It can be, for example, the North American Datum 1983 (NAD 83), the World Geodetic System 1984 (WGS 84), or any local datum, such as State Plane Coordinate System 1983, or any local system established for the purpose of a mapping project. The relationship between the navigation frame and the ECEF frame, which can be considered here as an example of a mapping frame, is shown in Figure 1.6.

#### 1.4.4 The Body Frame

The body frame is an orthogonal axis set, which is aligned with the roll, pitch, and heading axes of a vehicle. The body frame is used to define the roll, pitch, and heading of the vehicle, represented by  $\omega$ ,  $\phi$ , and  $\kappa$ , respectively. Since the INS is the only sensor inside the vehicle, it was oriented so that its x, y, and z axes would correspond with the x, y, and z axes of the vehicle body frame. From this point forward, the INS body frame and the vehicle body frame will be considered the same. The body frame is illustrated in Figure 1.7 and the individual rotations are illustrated in Figure 1.8.

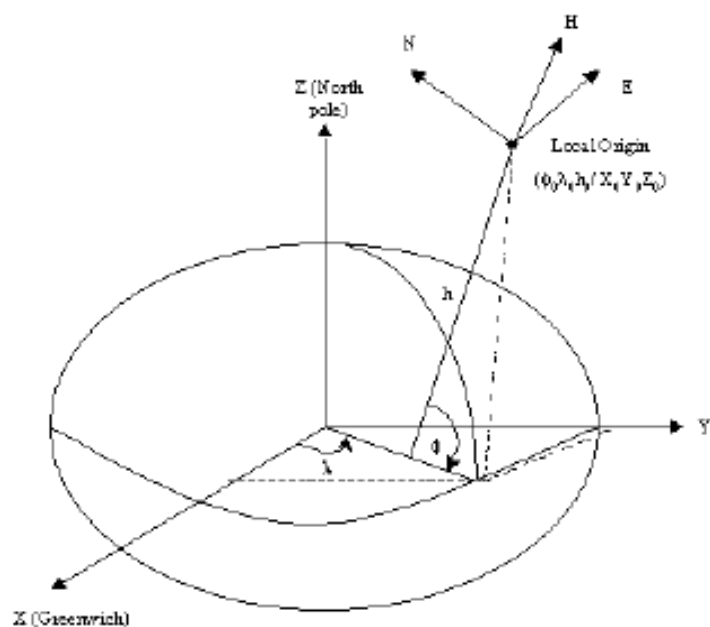


Figure 1.6: The ECEF Frame and the Navigation Frame. The ellipsoid represents the Earth with the origin of the X, Y, and Z axes of the ECEF system fixed at its center of mass. A point in this system is represented by longitude ( $\lambda$ ), the angle turned counter-clockwise from the x-axis, latitude ( $\phi$ ), the angle between the XY plane and a line normal to the ellipsoid, and a height ( $h$ ) above the ellipsoid. The navigation frame is situated at the local origin and is offset from the ECEF origin by three translational offsets  $X_0, Y_0, Z_0$  and three rotational offsets  $\phi_0, \lambda_0, h_0$ .

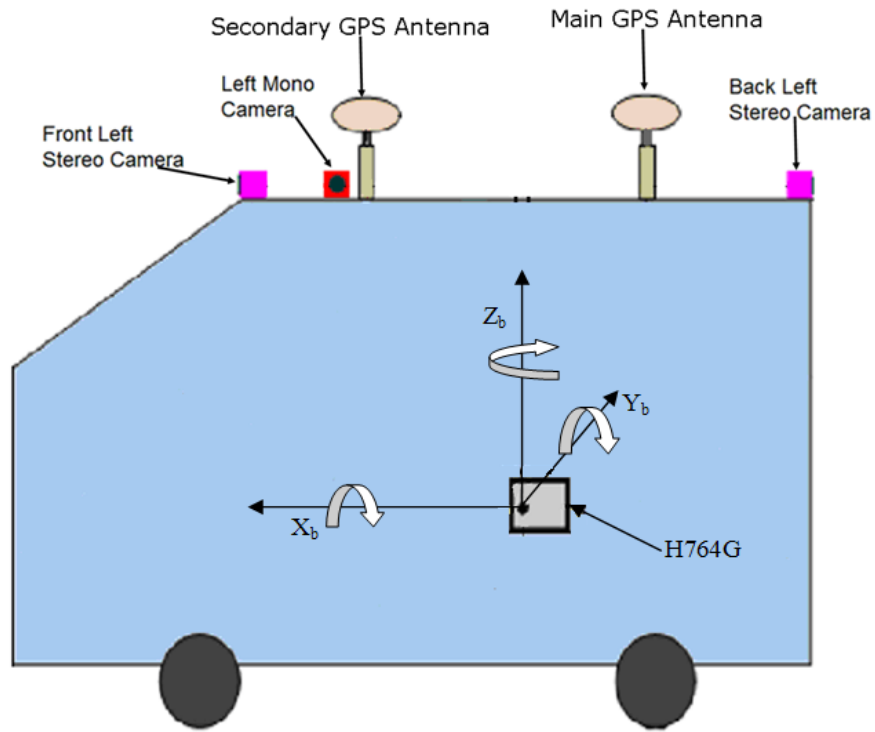


Figure 1.7: Body Frame Definition. This figure shows the definitions of the body frame axes within the GPSVan. In the figure above, the  $Y_b$ -axis is going into the figure, and the arrows show the directions of the rotation for attitude angles: roll ( $X_b$ -axis), pitch ( $Y_b$ -axis) and heading ( $Z_b$ -axis); see also Figure 1.8.



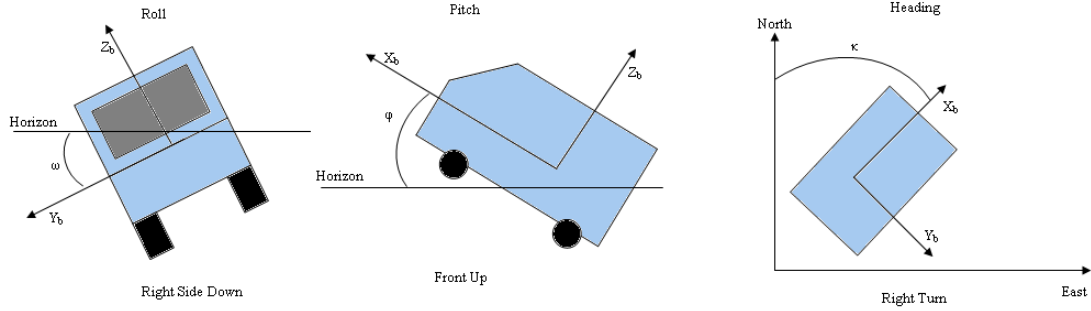


Figure 1.8: Body Frame Rotations. Rotations in the body frame include roll ( $\omega$ ) about the  $X_b$ -axis, pitch ( $\varphi$ ) about the  $Y_b$ -axis and heading ( $\kappa$ ) about the  $Z_b$ -axis.

#### 1.4.5 Photo Coordinate System

The photo coordinate system is a two-dimensional coordinate system as shown in Figure 1.9. In this coordinate system, the image fiducial marks or photo reference marks around the camera frame define the center of collimation or fiducial center based on the intersection of lines between fiducial marks directly across the image from each other. For convenience, the fiducial center will be taken as the origin of the image and will define the  $x$  and  $y$  axes along with the fiducial marks. However, the photo coordinate system is only a temporary coordinate system and one of the goals of camera calibration is to replace the fiducial center with the calibrated Principal Point. The Principal Point is mathematically defined as the foot to the perpendicular dropped from the perspective center to the plane of the photograph (Figure 1.9). The perspective center is one through which all points are projected onto the reference plane. The Principal Point is determined during camera interior orientation calibration and is assumed to lie on the  $z$ -axis in the positive direction. Since the Principal Point marks the true origin of the photo coordinate

system each point will then be able to be represented by an XY position in the two-dimensional photo coordinate system.

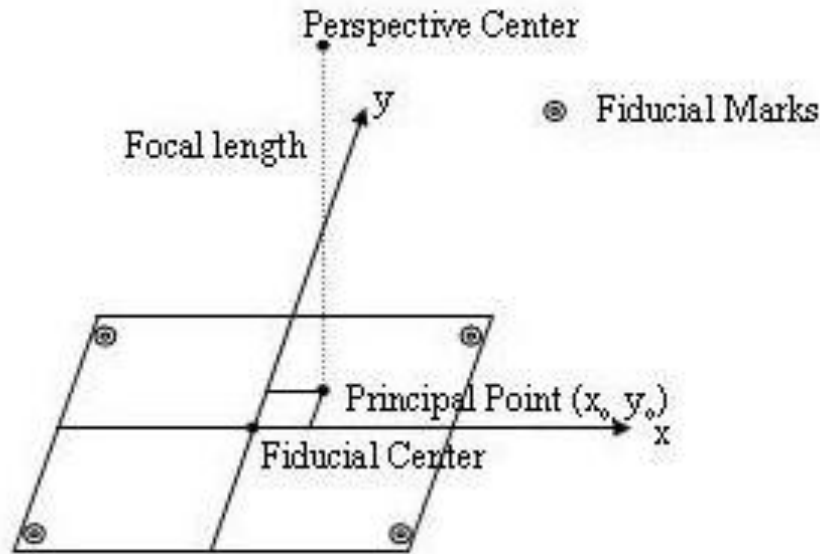


Figure 1.9: The Photo Coordinate System. This figure represents the fiducial center in the center of the image found by the intersection of the fiducial marks around the edges and shows that this does not necessarily correspond with the Principal Point. The Principal Point is the foot of the perpendicular dropped from the perspective center to the plane of the photograph and is the true origin of the photo coordinate system.

#### 1.4.6 Image Coordinate System

A photograph is a two-dimensional representation of a three-dimensional object space. This coordinate system is centered at the perspective center of the camera with the x-axis generally chosen in the direction of movement. The y and z axes will complete a right handed coordinate system, with the z-axis pointing out of the image. This will allow any point on the image with photo coordinates (x, y) to be represented with the image coordinates (x, y, f), where f is the focal length of the camera that is equivalent to

the distance from the camera perspective center to the image plane. The image coordinate system is depicted in Figure 1.10.

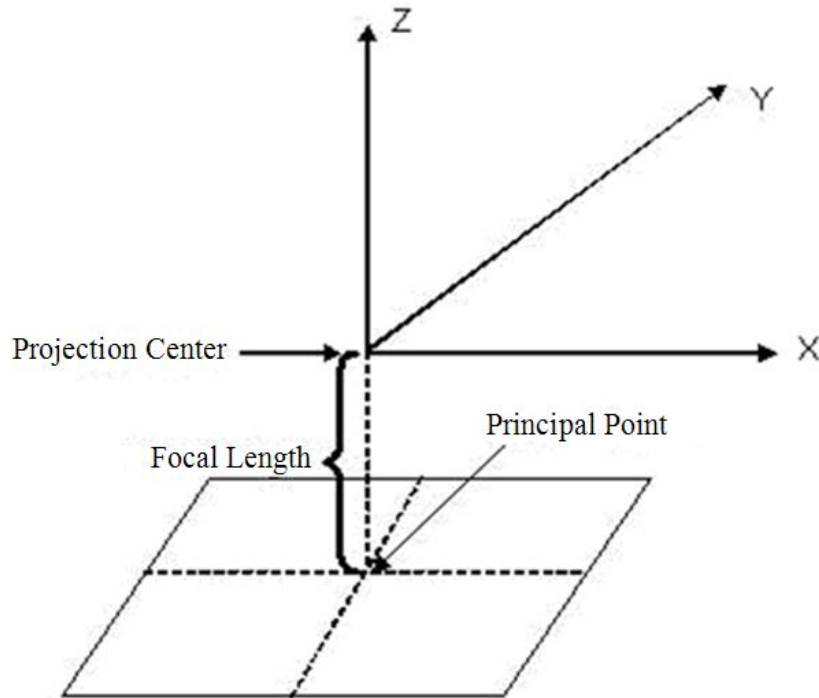


Figure 1.10: Image Coordinate System. The orientation of the image coordinate system is shown with respect to an image. The origin of the image coordinate system is offset from the Principal Point by the focal length.

## 1.5 Overview

This thesis consists of four chapters. Chapter 1 gives an introduction to the need for sensor calibration and explains the basics of the sensors to be used in the calibration process described here. This chapter then defines commonly used earth models and the reference frames used by the sensors. Chapter 2 deals with lever arm determination amongst the sensors. This chapter has a particular emphasis on the surveying techniques

used to determine the relative sensor positions and determination of the GPS/INS lever arm. The determination of camera lever arms will be described in this chapter as well, but these are temporary lever arms, and the actual lever arms cannot be resolved until the final camera exterior orientations are computed. Chapter 3 deals with determining camera orientation. Specifically, this chapter will determine the position and orientation of the camera perspective center with respect to INS body frame for each camera and determine the change in orientation between the stereo cameras through contemporary photogrammetric techniques. Finally, chapter 4 presents conclusions regarding the multi-sensor calibration process.

## Chapter 2 Lever Arm Determination

### 2.1 Introduction

As mentioned earlier, the data gathered by the sensors, mounted in the GPSVan, must all be related to a common reference frame, if consistent mapping information is to be obtained. For instance, the GPS and INS are complementary sensors for determining position and attitude angles at a given time. Positional information is obtained using GPS and INS together in environments where both are available, and INS is used by itself during the periods of GPS loss of lock. The INS will always be used to calculate position coordinates and attitude angles, but its IMU sensor errors must be calibrated by GPS to correct for time dependent drifting in the solution. The dual use of these sensors is particularly common in urban environments and it may be required to constantly switch back and forth between them, as losses of GPS lock are frequent in these environments. In order to benefit from GPS and INS complementary characteristics, both sensor solutions must be referring to the same point, so that there can be a smooth transition between sensors for determining navigation solutions. Otherwise, these sensors will each record data in their own reference frame; thus, linear offsets, referred to as lever arm offsets, between the GPS antenna phase center and the center of INS body frame, must be determined.

A similar situation arises for the cameras, which are dependent on an accurate and consistent determination of position and orientation (attitude angles) to properly georeference the images. Thus, an accurate navigation solution is needed for the georeferencing process. Additionally, the cameras must all be related to the point to which positional measurements are being referred (here, center of INS body frame). Otherwise, there is an offset between the location of the camera measurements and the location of the positional measurements, and accurate georeferencing is not possible.

To ensure accurate positional information, the reference frames of the GPS, INS, and six cameras will be related to a common reference frame, the INS body frame. Since the GPSVan is a kinematic platform whose navigation information is required, it will be used to define the navigation frame. Also, since the INS is the only sensor located inside the GPSVan, its body axes will be used to define the navigation frame to which all other sensors are related. The other sensors can be related to the navigation frame by computing the lever arms between the INS and the center of each sensor in the INS body frame. The lever arms consist of three linear offsets in the X, Y, and Z directions of the INS body frame to the sensor center. These offsets can be determined through precise surveying of each sensor center and then calculating the translational components from the INS center to the center of each sensor.

## 2.2 Sensor Survey

The Sensor survey was conducted using a Leica TS02 total station shown in Figure 2.1. The minimum angular precision was set to a tenth of a second and the minimum distance precision was set to a millimeter. The total station was operated

primarily in a reflectorless mode during data acquisition, allowing sensor positions to be recorded directly without having to model offsets from the center of the prism to each point measured on the sensors.



Figure 2.1: Leica TS02 Total Station. This image shows the total station used in the survey of the sensors and ground control points.

The survey can be divided into two parts: determining coordinates of critical (reference) sensor points and determining the position of ground control points. Determining the coordinates of critical sensor points will be used to find the center of the individual sensors and determine their spatial relationship to each other for use in determining the lever arms. The survey also included determining the position of ground control points to be used in a resection to determine the translational and rotational

offsets between the camera center determined in the survey and the actual camera center. This latter process will be discussed in more detail in chapter 3.

### *2.2.1 GPSVan Survey*

The survey of the GPSVan sensors was a relative survey, that is, a survey based on relative coordinates. Relative coordinates are defined within a local area and are taken with respect to the position of a single point. Unlike absolute coordinates, which are fixed in space and correspond to a single unique location, relative coordinates do not fix the location of an object in space. Rather, they show the spatial relationships among objects. Thus the coordinates of objects are known relative to a single fixed point in space. The point chosen for this purpose was a fiducial mark (see Figure 2.2), which was the fiducial mark in the top left corner, established in the control network shown in Figure 2.3. This network of fiducial marks was established for use in camera calibration and was setup along the I-beams inside the Center for Automotive Research (CAR) facility at OSU West Campus, so that they would be on a stable, unchanging location. This was needed because the top leftmost marker not only was the reference point for the survey, but the coordinates of all of these points were recorded and were later imaged by the cameras on the GPSVan to determine the camera interior orientation parameters. As a result, it was important to choose a location for the targets that would be as stable as possible. The fiducial marks in Figure 2.3 outlined in red were placed between the I-beams on soft wall composed of insulation and a thin covering. These points were originally intended to be used as optional points, but were discarded due to the possibilities of slight variations in the wall due to temperature changes. While it may



seem like a trivial matter, it is extremely important for camera calibration and the rest of the survey, because if the points are not stable, the camera calibration results will not be as accurate as possible and the relative position of the sensors will not be tied to a consistent point. An actual representation of the fiducial control point network is shown in Figure 2.4, detailing the differences between the stable I-beams and the soft and flexible walls.



Figure 2.2: Fiducial Mark from Control Network. A typical fiducial mark used in establishing the fiducial mark control network inside the Center for Automotive Research.

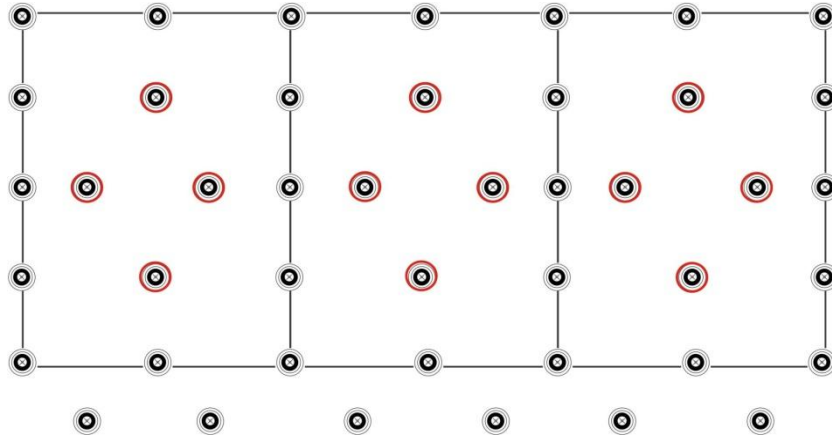


Figure 2.3: Entire Fiducial Mark Control Network Inside Center for Automotive Research.



Figure 2.4: Visual Representation of the Fiducial Control Network. This image depicts the differences between the I-beams and the soft wall where the fiducial control network was established to emphasize the difference in stability between the different surfaces.

With an established reference point from which all observations were made, the total station could then be setup at different locations around the GPSVan to record the coordinates of reference (critical) points on different sensors. The positions of setup were spaced around the GPSVan, and chosen so that redundant measurements of most sensors could be made from sequential locations as a verification of accuracy later on. The setup locations are shown with respect to the GPSVan in Figure 2.5 below. In this figure, orientation of the GPSVan with respect to the wall of control points and the orientation of  $x$  and  $y$  axes of the body frame are shown. Information about the sensor corresponding to each point number in Figure 2.5 is given in Table 2.1 below. Finally, the setup locations are next to the  $X$ 's on the ground marked with S1, S2, S3, and S4 corresponding to Station 1, Station 2, Station 3, and Station 4 respectively.

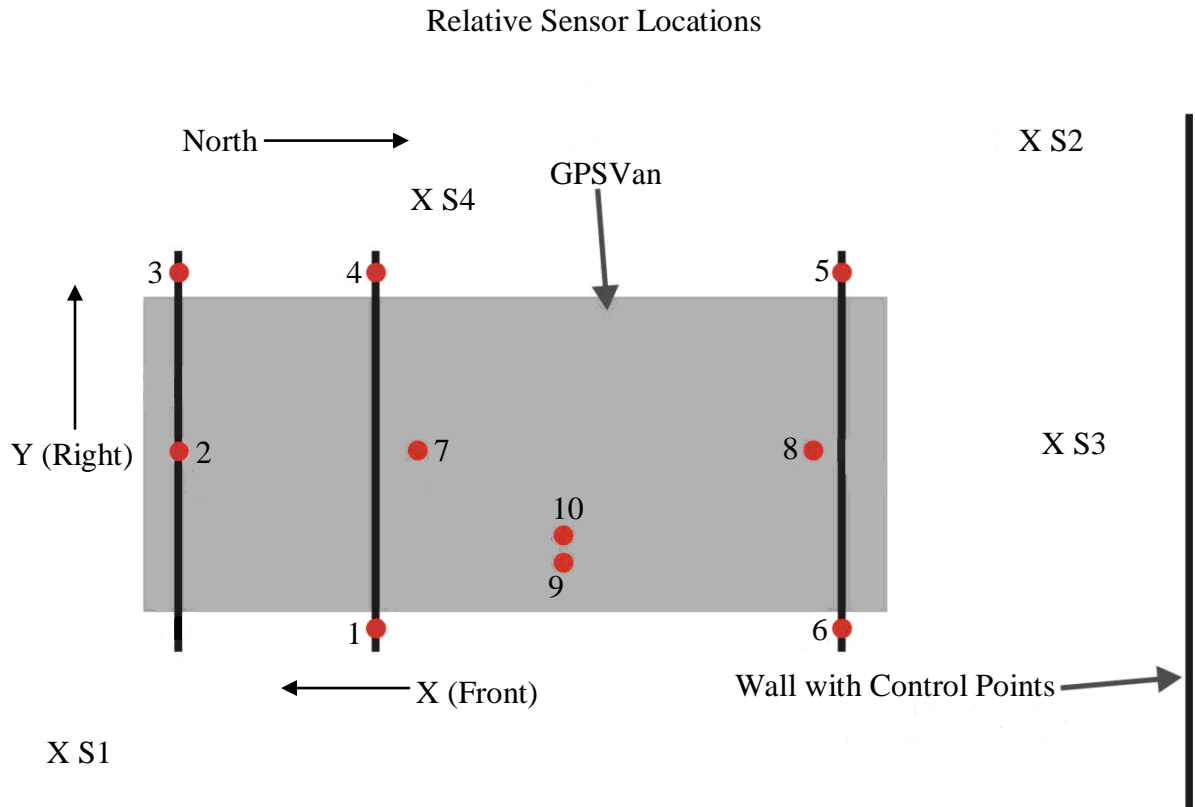


Figure 2.5: Setup Locations Relative to GPSVan. The red points numbered 1 to 10 represent the sensors on the GPSVan described in Table 2.1 below. The positive X and Y axes of the INS body frame are shown in the figure, and the positive Z-axis would be coming out of the figure. The wall with control points refers to the network of fiducial marks shown in Figure 2.3. All of the X's marked S1 through S4 represent the different locations where the total station was setup to record features on the GPSVan, proceeding numerically from S1 (Station 1).

Sensor Number	Type	Relative Location	Model
1	Camera	Middle Left	Prosilica
2	Camera	Front Left	Prosilica
3	Camera	Front Right	Prosilica
4	Camera	Middle Right	Prosilica
5	Camera	Back Right	Prosilica
6	Camera	Back Left	Prosilica
7	GPS Antenna 1	Middle	Topcon Legacy (GNSS) with 4-way splitter
8	GPS Antenna 2	Back	Topcon Legacy (GNSS) with 4-way splitter
9	Navigation Grade IMU	Left	H764G1
10	Navigation Grade IMU	Right	H764G2

Table 2.1: GPSVan Sensor Identification. The sensors numbers listed in Table 2.1 correspond to the red points in Figure 2.5.

After the total station was setup at each of the designated stations in Figure 2.5 it was first leveled. Upon completing the leveling, the height of the total station was measured three times, and the average was used as the instrument height at that particular station. The station position was found by backsighting to the top left fiducial mark, which was given an arbitrary default northing, easting, and height position. This northing, easting, and height system is a localized plane surveying coordinate system. The project area is small enough, so that the curvature of the earth will not impact the coordinate values. This local coordinate system is defined so that the positive x-axis is in the east direction, the positive y-axis is in the north direction, and the positive z-axis completes a right-handed coordinate system. Upon backsighting the reference fiducial mark, the relative coordinates of the total station position were determined by the distance from the total station to the center of the fiducial mark, the angle turned clockwise from north, and the zenith angle. The zenith angle is the angle measured downward from the vertical

plane, that is, a point directly overhead, to another point. Computation of the total station position from the backsight is illustrated in Figures 2.6 and 2.7. Backsighting also zeroed the angle on the top left fiducial mark, so all angles were turned with respect to it instead of north.

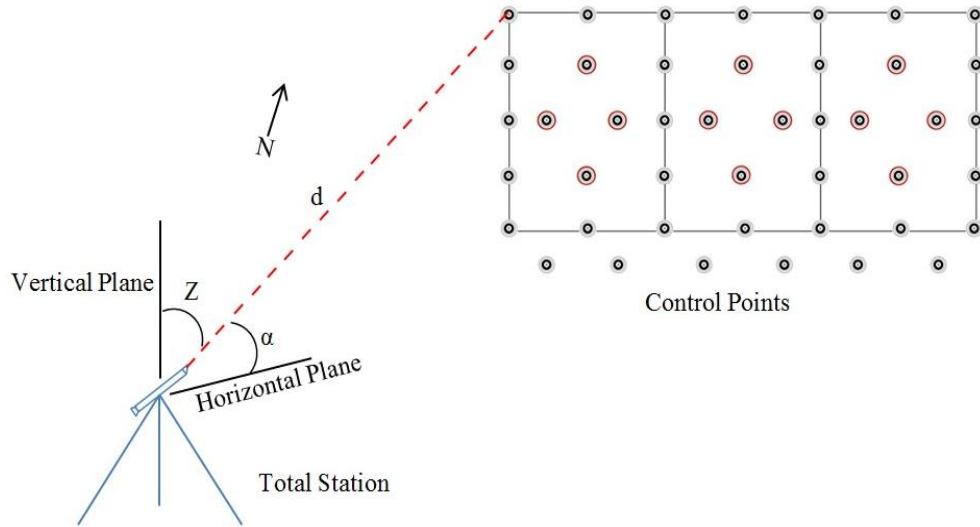


Figure 2.6: Distance and Zenith Angle Determination. The distance ( $d$ ) is the three-dimensional distance vector from the total station to the top left fiducial mark in the control network. The angle  $Z$  is the zenith angle, that is the angle measured from the vertical plane overhead to the top left fiducial mark, and the angle  $\alpha$  is the complement to the zenith angle. Here,  $N$  represents the direction of magnetic north.

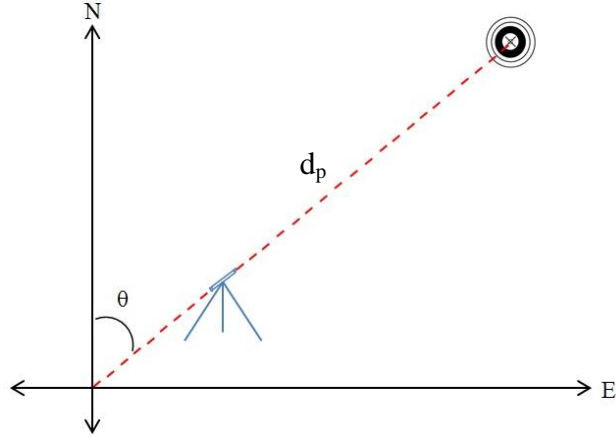


Figure 2.7: Northing and Easting Determination. The heading angle ( $\theta$ ) is the angle measured clockwise with respect to north in the horizontal plane shown in Figure 2.6. The distance  $d_p$  in this figure is the projection of the three-dimensional distance vector  $d$  in Figure 2.6 onto the horizontal plane.

In Figure 2.6,  $N$  represents the direction of north with respect to the total station setup,  $d$  is a three dimensional vector measured from the total station to the top left fiducial mark,  $Z$  represents the measured zenith angle and  $\alpha$  represents the verticle angle, the angle complimentary to the zenith. In Figure 2.7,  $\theta$  is the horizontal angle measured clockwise from north to the fiducial mark. With these two angles and the distance it is possible to use simple trigonometry to determine the change in coordinates between the total station and fiducial mark as follows:

$$dH = d \times \cos Z \quad (2.1)$$

$$dN = d \times \sin Z \times \cos q \quad (2.2)$$

$$dE = d \times \sin Z \times \sin q \quad (2.3)$$

Where

$dH$  is the change in height from the total station to the fiducial mark

$dN$  is the change in northing from the total station to the fiducial mark

$dE$  is the change in easting from the total station to the fiducial mark

$d$  is the three-dimensional distance vector from the total station to the measured point

$Z$  is the zenith angle measured from the vertical to point being measured

$\theta$  is the angle measured clockwise from north in the horizontal plane

Since  $dH$ ,  $dN$ , and  $dE$  describe the change in coordinates from the total station to the fiducial mark, the opposite of these changes can be added to the coordinates of the fiducial mark to obtain the coordinates of the total station. At this point, the position of the total station is known in the relative coordinate system and is defined by a northing, easting, and height, corresponding to the measurement center of the total station. This same procedure was used each time the total station was setup at a new station to compute the relative coordinates of that station, so that all resulting sensor measurements would be in the same relative coordinate system.

With the relative coordinates of the total station known, precise measurements could then be made to obtain the coordinates of the center of each sensor or reference points. The sensor coordinates are determined by calculating the change in height, northing, and easting between the total station and the point on the sensor being measured and directly adding these changes to the height, northing, and easting coordinates of the total station. However, the center of all the sensors could not be directly measured, so points were chosen around each sensor and used to determine the sensor center. A brief description of how the center for each sensor was calculated and the rationale behind choosing the sensor measurement follows.

The measurement center for the GPS antennas is the the antenna phase center. This is a point located inside the antenna and can be determined by manufacturer specifications with reference to certain external points, such as the antenna base plane. For this reason, the base plane of the antenna was chosen as a high priority point to measure. The other point chosen was the base of the thread on the extender to which the antenna attaches. This was chosen as a convenient point to verify the distance from the base of the thread to the position on the thread where the bottom of the GPS antenna sits and the antenna base plane lays. Figure 2.8 shows a view of sensor 8, the rear GPS antenna, from the left side of the GPSVan and illustrates the points surveyed. This figure does not include the GPS antenna for clarity of seeing the point measured at the base plane.

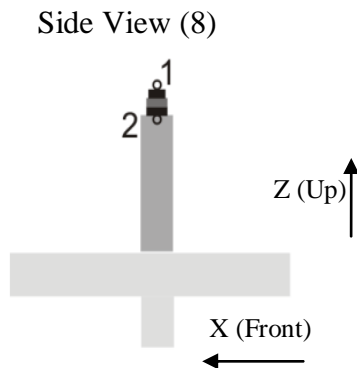


Figure 2.8: Main Antenna Survey Points. Points 1 and 2 are the points surveyed to on the main antenna. Refer to sensor number 8 in Table 2.1 for specific information regarding this sensor, and Figure 2.5 for its location on the GPSVan. The orientations of the positive X and Z axes of the INS body frame are shown and the positive Y-axis would be going into the figure.



Similarly to the GPS antenna, the center of the INS is internal. However, unlike the GPS antenna the center of the INS body frame can be represented as a point inside the INS with a location, specified by the manufacturer, with respect to the distinct points on the chassis. In this case, the bolts on the top of the chassis were specified as the reference point from which the the center of the INS would be determined. The bolts were somewhat recessed in the chassis, so they could not be accurately surveyed from the field of view available. Instead, four points were surveyed on the side of the INS and used to determine the position of the bolts. Figure 2.9 shows the points surveyed on the front (positive x-axis) side of the INS from Station four. Points three to six are the points surveyed and used to determine the the location of the two front bolts. In Figure 2.9, the chassis is represented by the dark gray encasing H764G1 and H764G2. There are bolts on the top of the chassis where the vertical members join the top plate. The position of points three and five were surveyed and the location of the bolts was calculated through additional hand measurements. Points four and six were chosen as a check of the results of points three and five and the same procedure was applied to them. The center of the bolts was then determined through these surveyed points and the additional measurements relating them to the center of each bolt. Then, the INS blueprints are used to specify the location of the INS body center along axes x, y and z that are parallel to the orthogonal faces of the INS.

Like the GPS, the camera centers cannot be found through survey data alone. Instead, they will be determined later through a resection discussed in chapter 3. The survey assumes that the camera lens center will serve as a approximate sensor center for

each camera. This center can be found through the intersection of lines drawn through the lens from three precisely surveyed points around the lens circumference. Figure 2.10 shows the points chosen around the lens circumference for the front two cameras (sensors 2 and 3 in Table 2.1). This is a view looking at these sensors from the front of the vehicle. In this case, the center was found by the intersection of a horizontal line created from a point on the side of the camera lens and a vertical line created between a vertical point at the top and bottom of the lens. While this can provide an accurate center after data processing it assumes that the surveyed points were precisely ninety degrees apart along the circumference. As such this method of determining center has a greater chance of error to enter the calibration process. A more accurate and more computationally intense method of computing the temporary camera center is to use three points randomly dispersed around the circumference and determine the point of intersection of these lines within the circle. Regardless of the method used to find the lens center, it will be used as an initial approximation of the camera center for the camera resection discussed in chapter 3.

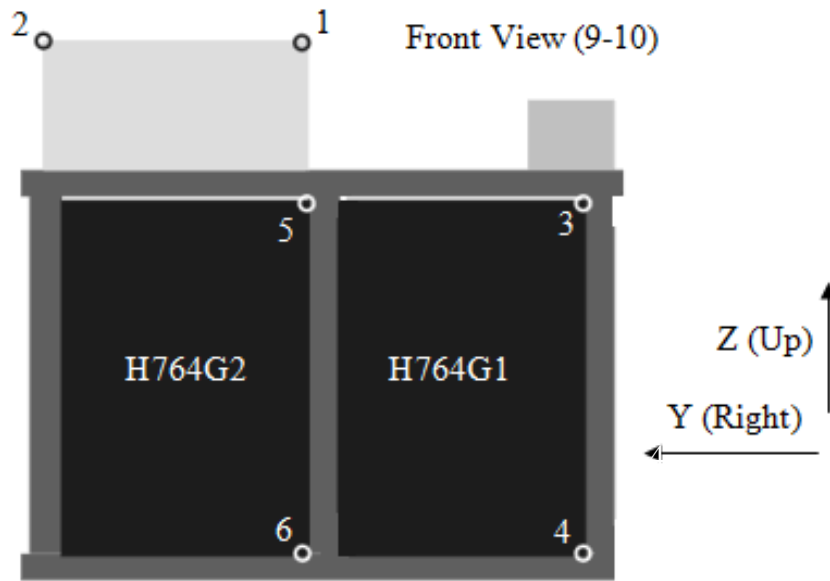


Figure 2.9: INS Survey Points. Points 1 to 6 show the surveyed positions of the INS. Specifics about this sensor can be found by sensor numbers 9 and 10 Table 2.1 and the positions of these sensors are shown as points 9 and 10 in Figure 2.5. The orientation of the positive Y and Z axes of the INS body frame are shown in this figure and the positive X-axis would be coming out of the figure.

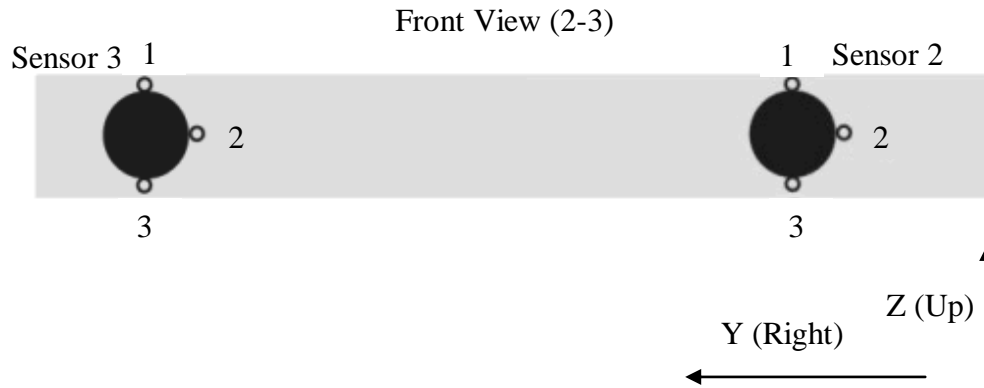


Figure 2.10: Camera Survey Points. Points 1, 2, and 3 around sensors 2 and 3 represent the survey points used to find the geometric center of each camera lens. Specifics for these sensors are shown as sensor numbers 2 and 3 in Table 2.1 and the positions of these sensors are shown by points 2 and 3 in Figure 2.5. The orientation of the positive Y and Z axes of the INS body frame are shown and the positive X-axis would be coming out of the figure.

### 2.2.2 Ground Control Point Survey

Ground control points were established inside and outside of the CAR facility. The points inside used the fiducial network established on the I-beams and the points outside consisted of rivets on the sheet metal wall. A very similar procedure was used in both cases: determine the relative coordinates of the points from a reference point or reference station, then tie the surveyed points to absolute coordinates. Since establishing the exterior ground control points jointly deals with the setup of stations used for absolute positioning, it will be discussed first.

The wall of exterior control points is shown in Figure 2.11, with the surveyed rivets circled in red. Prior to the survey, a baseline approximately twenty meters in

length was defined more-or-less parallel to the wall and offset eight meters north on the west end and ten meters north on the east end. The total station was setup over the eastern endpoint of this baseline, it was leveled, and its height was computed by taking the average of three measurements. A prism pole was then set so the center of the prism would be the average height of the total station measurements, and it was used to occupy the western endpoint of the baseline, which is serving as the reference station in this survey. Just as with the sensor survey on the GPSVan, the reference station was given arbitrary coordinates, the average height was input for the station height and a backsight was taken to the prism pole on the reference station to determine the relative coordinates of the eastern endpoint line from which all rivets were surveyed. The rivets were then surveyed beginning in the top left corner and proceeding right in a snake-like pattern to the lower left corner.

The relative coordinates of the interior network of fiducial marks were determined in the same manner as the sensors on the GPSVan. After setup, the fiducial mark in the top left corner was backsighted, tying the coordinates of the total station and subsequent measurements to the same relative coordinate system as the GPSVan sensors. Once the absolute coordinates of the top left fiducial mark are known, the absolute coordinates of all other interior points (GPSVan sensors and fiducial mark coordinates) can be calculated by adding the change in relative coordinates from the top left fiducial mark to another fiducial mark or sensor to the absolute coordinates of this fiducial mark.



Figure 2.11: Exterior Ground Control Points. The rivets circled in red were surveyed on the outside northern wall of the Center for Automotive Research to be used as ground control points. That is, points with a unique three-dimensional coordinates used as an absolute reference.

Prior to establishing absolute coordinates, another baseline, approximately seventeen meters long, was established beginning at the eastern endpoint of the first baseline and extending south ten meters and east fourteen meters. The endpoint of the second baseline was carefully chosen, so that it would be visible from the point of beginning as well as visible through the bay door of the CAR facility and so that the area surrounding the endpoint would be as open as possible to minimize GPS obstructions. Afterwards, the western endpoint of the first baseline, the southeastern endpoint of the second baseline, and the middle point common to both baselines were occupied using a Novatel Nov702GG GPS antennas to obtain the absolute coordinates of these points.

Prior to GPS occupation and backsighting, magnails were driven into the asphalt to mark the location of the three endpoints defining both baselines. GPS occupation was

then done by setting up, centering, and leveling tripods on which to mount the antennas over the magnails. At the end of the GPS observation period, the GPS coordinates of each of the stations were processed using OPUS, the online positioning service from the National Geodetic Survey <<http://www.ngs.noaa.gov/OPUS/>>. With this step completed, the X, Y, and Z coordinates of the GPS stations are known and must be related to the ground control points. This is done by dropping the height of the GPS antenna to the ground to obtain the coordinates of the magnail and using the height of the total station to relate its position to the absolute position of the magnail. Since the height of the GPS antenna was recorded after it was setup, and since it was measured from the center of the magnail, this distance can then be subtracted from the height in the OPUS solution to determine the X, Y, and Z coordinates of the center of the magnail. Since the total station was centered over the magnail and its height was recorded prior to beginning the survey this height can be added to the height of the center of the magnail to obtain the height of the total station.

At this point, the absolute X, Y, and Z coordinates of the total station are known. A similar process must be repeated with the western endpoint and the height of the prism pole to determine the absolute coordinates of the backsight used for the survey. Since the angle was zeroed on the backsight target, all angles were relative angles, turned with respect to the backsight as zero degrees or magnetic north. The backsight must now be rotated with respect to north back to its proper azimuth and this same rotation must be applied to angles turned from the backsight. This process can be done using inverse coordinates as follows:

$$\text{Bearing} = \tan^{-1}((E_1 - E_2)/(N_1 - N_2)) \quad (2.4)$$

Where

$E_1$  and  $E_2$  are the easting coordinates of backsight and station occupied, respectively.

$N_1$  and  $N_2$  are the northing coordinates of the backsight and station occupied, respectively.

In equation 2.4, the bearing is determined in degrees in one of four quadrants: north and east, south and east, south and west, or north and west. Bearings are the smallest horizontal angle that a line makes with a north or south meridian and cannot have a value larger than ninety degrees, which would correspond to due east or west. Consequently, every bearing exists within a particular quadrant of a circle which must be determine to know the orientation of the bearing with respect to zero degrees or magnetic north. The appropriate quadrant is determined by the difference in northing and easting coordinates. If the differences in northings and eastings are both positive the bearing will be in the northeast quadrant, if the difference in northings are negative while the difference in eastings are positive the bearing will be in the southeast quadrant, if the differences in northings and eastings are both negative the bearing will be in the southwest quadrant and if the difference in northings is positive and the difference in eastings is negative the bearing will be in the northwest quadrant.

Prior to rotating the backsight point and all angles back to their proper azimuth the calculated bearing will be converted into an azimuth for simplicity. An azimuth is a



horizontal angle measured from the north and is measured as a full circle unlike a bearing. The conversion from bearings to azimuth is as follows:

If the bearing is north and east

$$\text{Azimuth Value} = \text{Bearing Value} \quad (2.5)$$

If the bearing is south and east

$$\text{Azimuth Value} = 180^\circ - \text{Bearing Value} \quad (2.6)$$

If the the bearing is south and west

$$\text{Azimuth Value} = 180^\circ + \text{Bearing Value} \quad (2.7)$$

If the bearing value is north and west

$$\text{Azimuth Value} = 360^\circ - \text{Bearing Value} \quad (2.8)$$

With the azimuth known the rotation between the backsight and north is then computed as:

$$\text{Rotation} = 360^\circ - \text{Azimuth Value} \quad (2.9)$$

The rotation value calculated in equation 2.9 is the value which must be subtracted from all angles turned from the backsight, so that the angles turned from the backsight to each point will correspond to their proper azimuth with respect to north.

With the northing, easting, and height of the backsight and total station known, as well as the azimuths of each control point, distances of from the total station to each control point, and azimuths from north to each control points the absolute coordinates of the control points can be calculated using equations 2.1, 2.2, and 2.3. Afterwards, the coordinates of all the control points are unique and fixed in space, unlike the relative

coordinates which are arbitrary and free-floating around the backsight since there is nothing to control the orientation of the points.

The same procedure is used to determine the absolute position of the sensors and control points inside the CAR facility. In doing so, the total station was first setup over the southeast endpoint of the second baseline. Upon leveling and measuring the height, a backsight was taken to the prism pole on the magnail at the other end of this baseline. A location was then selected inside which would offering a view of the fiducial targets and from which the total station could also be seen, and a fiducial target was placed on the floor to mark the location. The prisim pole was then setup over this target and its relative position was determined with respect to the last backsight. The bearing from the southeast endpoint to the northwest endpoint of the second baseline was calculated, and the rotation angle was calculated after converting it to an azimuth. After applying this rotation, the absolute coordinates of the fiducial mark placed on the ground could be computed in the same manner as the absolute coordinates of the control points on the outside.

The total station was then moved inside the CAR facility and setup, leveled and the hieght was recorded over the fiducial mark on the floor. The prism pole was then used to backsight the southeast endpoint of the second baseline and a measurement was taken to the top left fiducial mark. The absolute coordinates of this point were then computed using the same procedures as above with the current total station location and southeast endpoint as the baseline. Measurements were also taken to the other four

stations so that the absolute coordinates of these stations could be computed using the same rotational offset.

At this point, each of the absolute coordinates of each of the stations are known, as well as the absolute coordinates of the top left fiducial mark used as the backsight. A baseline can now be formed between the top left fiducial mark and each station, and the rotation corrections for each station can be calculated and applied to all measurements made from that station. The absolute coordinates can now be computed for each fiducial mark in the newtwork as well as for all measurements on the GPSVan sensors.

### 2.3 Lever Arm Computation

The sensor level arms of the GPSVan can be calculated now that the absolute coordinates of all points are known. All lever arm computations will be made with respect to the H764G1 INS, which is the left INS in the dual INS system used, which is located inside the GPSVan, as previously mentioned. The primary level arm to be determined is the GPS/INS lever arm, determining the translational offsets between the INS center of the body frame and the GPS antenna phase center in the INS body frame. This lever arm will be computed using the measurements of the H764G1 INS, as the origin of the INS body frame, and the phase center of the main antenna (sensor 8 in Table 2.1). The linear offsets will be determined by the difference in the northing, easting, and height coordinates of the INS body frame origin and the GPS antenna phase center. The signs of the translation magnitudes will be determined from the origin of the INS body frame as follows: positive translations are to the right (passenger's side), towards the

front, and up, while negative translations are to the left (driver's side), towards the back, and down. The same procedure is then used to determine the approximate lever arm for each of the six cameras, and the lever arm of the remaining GPS antenna. The approximate lever arms for each camera will be used as an initial approximation of the coordinates of the camera perspective center for each camera for the resection discussed in chapter 3. Figures 2.12 and 2.13 depict the driver's side view and back view of the GPSVan respectively. The lines in the figures depict the survey vector components that determine mutual relationship among the sensors. The lever arm components between the INS and the GPS, and the six cameras are listed in Table 2.2

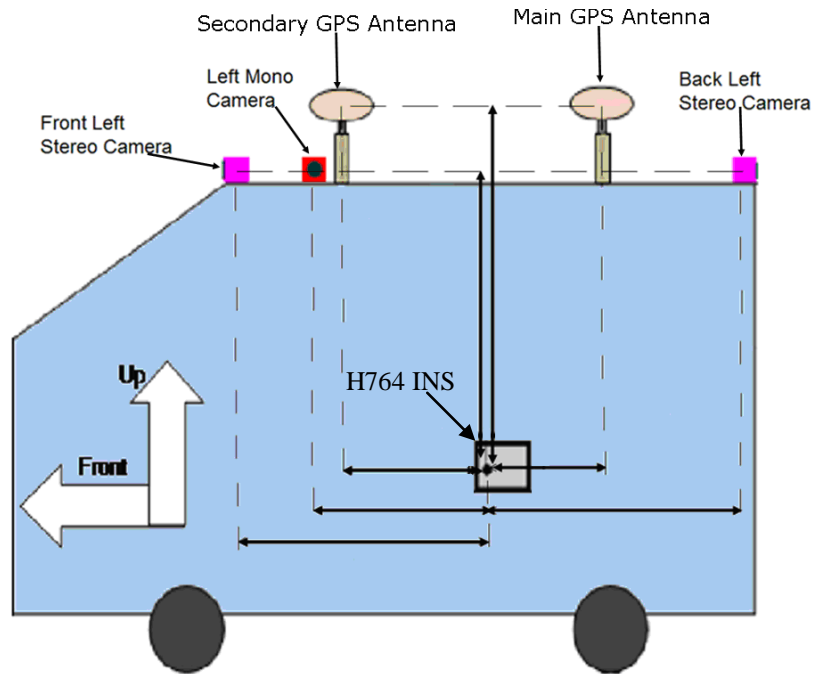


Figure 2.12: Driver's Side View of Lever Arm Components. All lever arm components are computed with respect to the H764G INS. The dashed lines in this figure represent the lines measured to the center of each sensor, and the bold arrows depict the survey vector components that determine mutual relationships among the sensors. The lever arm components were calculated as right, front, up components, corresponding to the positive Y, X, and Z axes of the INS body frame, respectively. The orientation of the positive Y-axis (Right) would be into the figure. Results of the lever arms are shown in Table 2.2.

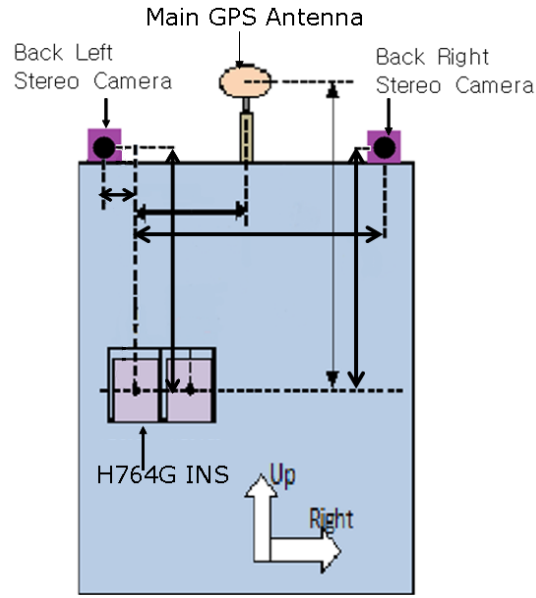


Figure 2.13: Rear View of Lever Arm Components. All lever arm components are computed with respect to the H764G INS. The dashed lines in this figure represent the lines measured to the center of each sensor and the bold arrows depict the survey vector components that determine mutual relationships among the sensors. The lever arm components were calculated as right, front, up components, corresponding to the positive Y, X, and Z axes of the INS body frame respectively. The orientation of the positive X-axis (Front) would be into the figure. Results of the lever arms are shown in Table 2.2.

Sensors	Instrument	Right (m)	Front (m)	Up (m)
9 to 8	GPS/INS	0.454	-0.746	1.344
9 to 1	Middle Left Camera	-0.486	1.612	1.152
9 to 2	Front Left Camera	0.747	2.12	1.13
9 to 3	Front Right Camera	1.33	2.116	1.133
9 to 4	Middle Right Camera	1.33	1.595	1.163
9 to 5	Back Right Camera	1.291	-0.942	1.029
9 to 6	Back Left Camera	-0.459	-0.927	1.019

Table 2.2: Sensor Lever Arm Components. Information about each sensor can be found by its sensor number in Table 2.1 and the position of each sensor is shown on the GPSVan by the corresponding point in Figure 2.3.

## Chapter 3 Camera Inter-relationships

### 3.1 Introduction

As previously mentioned, the camera calibration consists of two parts: determination of the interior orientation parameters and derivation of the boresight transformation matrix and linear offsets that are required to obtain the six exterior orientation parameters (three defining the three-dimensional coordinates and three defining the orientation of the camera perspective center in the mapping frame) from the GPS/INS integrated system. Determination of the interior orientation parameters was done independently of this research and will, therefore, not be discussed in detail in this thesis. These parameters were determined by images taken of the established fiducial network whose three-dimensional coordinates were acquired during the survey. Images were taken from each camera from different positions and orientation with respect to this fiducial network and the two-dimensional points of the fiducial targets in the images were processed along with the absolute three-dimensional position of the targets using photogrammetric techniques to recover the camera interior orientation parameters. However, the interior orientation parameters were made available, as certain interior parameters are needed in the determination of exterior orientation parameters.

With the interior parameters known, all that remains of the camera calibration is the determination of the boresight transformations. This process will consist of two major parts: determination of the boresight transformation between the INS and each camera, and the determination of the boresight transformation between the left and right stereo cameras for both pairs of stereo cameras. The first part will be accomplished through the use of a photogrammetric resection to determine the exterior orientation parameters of the image. Once these are known, it is possible to separately determine the translational and rotational offsets between the cameras and the INS body frame. The second part, also known as a relative orientation, so called because it is determining the orientation of one camera with respect to the known position and orientation of another, will be used to define the offsets of individual stereo cameras in a process very similar to that used in determination of the boresight offsets for the lever arms.

## 3.2 Boresight Transformation

### *3.2.1 Introduction*

The GPS/INS lever arm was calculated in chapter 2, and allows for the ECEF position coordinates of the GPSVan to be determined at anytime by the GPS/INS system. Additionally, lever arms calculated in chapter 2 relate the geometric center of each camera lens to the INS center of the body frame. The lever arms between the cameras and INS can then be applied to find the position of the camera center, with respect to the origin of the INS body frame, for each camera at the moment of exposure. These lever arms were based on the geometric center of the lenses, which do not necessarily



correspond to the center of the image and, therefore, cannot be taken as the camera perspective center. The camera perspective center is the single point at which all light rays from three-dimensional objects in the object space would converge, if they were extended beyond the image plane. Additionally, the principle point in an image is defined by the location of the perspective center projected down onto the image plane. Therefore, the perspective center will be used to represent the true center of the camera and the exterior orientation parameters for this point will be determined for each camera. Once the position and orientation of the perspective center is determined through a resection, the orientation and position of both the perspective center and the INS body frame are known at the moment of exposure, and it is possible to compute the lever arm between the two.

### *3.2.2 Correcting Camera Lens Distortion*

The resection will be performed using points in the image coordinates of ground control points visible in the images as well as the coordinates of the corresponding ground control points. Prior to the resection, all of the selected image points must be processed to remove radial distortions caused by the camera lens. The lens distortion correction will be applied to each of the selected image points on a point by point basis.

The first step in this process is the computation of the maximum radial distance in the image. This is defined as the maximum of the distances from the Principal Point to each of the four image corners and can be calculated as:

$$r_{\text{max}} = \sqrt{(x_i - x_0)^2 + (y_i - y_0)^2} \quad (3.1)$$

Where

$r_{\text{max}}$  is the radial distance between the Principal Point and a given corner.

$x_0$  and  $y_0$  are the pixel coordinates of the camera principal point.

$x_i$  and  $y_i$  are the pixel coordinates of an individual corner.

This procedure is done using each image corner and the maximum distance is used. Each of the selected image points is then centralized by applying the Principal Point, so that the origin is the center of the image instead of the top left corner of the image as follows:

$$x_p = x_i - x_0 \quad (3.2)$$

$$y_p = y_i - y_0 \quad (3.3)$$

Where

$x_p$  and  $y_p$  are the pixel coordinates of a point based on an origin centered at the principal point.

$x_0$  and  $y_0$  are the pixel coordinates of the camera Principal Point.

$x_i$  and  $y_i$  are the pixel coordinates of an individual corner.

The advantage of this translation is that the pixel coordinates of an image point is a vector whose origin is at the Principal Point. This simplifies the calculation of the radial distance of an image point from the Principal Point given as:

$$r = \sqrt{(x_i - x_0)^2 + (y_i - y_0)^2} \quad (3.4)$$

Where  $r$  denotes the radial distance of an image point from the Principal Point.

$x_0$  and  $y_0$  are the pixel coordinates of the camera Principal Point.

$x_i$  and  $y_i$  are the pixel coordinates of an individual corner.

Next, the lens distortion parameters and overall radial distortion error can be calculated as:

$$c1=1/r\_max^2 \quad (3.5)$$

$$c2=1/r\_max^4 \quad (3.6)$$

$$c3=1/r\_max^6 \quad (3.7)$$

$$dr = c1 \times k1 \times r^2 + c2 \times k2 \times r^4 + c3 \times k3 \times r^6 \quad (3.8)$$

Where

$c1$ ,  $c2$ , and  $c3$  are lens distortion parameters.

$dr$  is the radial distortion error.

$k1$ ,  $k2$ , and  $k3$  are defined in the camera intrinsic parameters computed independently of this research.

The lens distortion in each direction can then be calculated as:

$$dx = dr \times x_p \quad (3.9)$$

$$dy = dr \times y_p \quad (3.10)$$

Where  $dx$  and  $dy$  are the lens distortion in the x and y directions, respectively for a given image point.

$dr$  is the radial distortion error.

$x_p$  and  $y_p$  are the pixel coordinates of a point based on an origin centered at the Principal Point.

The undistorted image point can then be calculated as:

$$X_{pp} = x_p + dx \quad (3.11)$$

$$Y_{pp} = y_p + dy \quad (3.12)$$

Where  $X_{pp}$  and  $Y_{pp}$  are the undistorted x and y coordinates of the image point.

$dx$  and  $dy$  are the lens distortion in the x and y direction for a given image point.

$x_p$  and  $y_p$  are the pixel coordinates of a point based on an origin centered at the Principal Point.

Finally, the undistorted image points are translated so that the origin is once again at the top left pixel of the image by adding the principal point back to each image point:

$$X_i = X_{pp} + x_0 \quad (3.13)$$

$$Y_i = Y_{pp} + y_0 \quad (3.14)$$

Where  $X_i$  and  $Y_i$  are the undistorted x and y pixel coordinates of an individual image point.

$X_{pp}$  and  $Y_{pp}$  are the undistorted x and y coordinates of the image point.

$x_0$  and  $y_0$  are the pixel coordinates of the camera Principal Point.

This process is then repeated for the remaining images points in each image and must be repeated for all images from each camera for which a resection is being done.

### 3.2.3 Image Resection

The camera perspective center will be determined through a resection, which is the process of registering and matching two-dimensional points in the image to their corresponding three-dimensional object space coordinates. This process is illustrated in Figure 3.1. Note that the position of the perspective center can be found by the convergence of the rays from the points in the object space to the points in the image. This will determine the coordinates of the camera perspective center, denoted here as  $X_L$ ,  $Y_L$ , and  $Z_L$ . Also notice in the figure that the camera will have an arbitrary rotation with

respect to the ground control points. These rotations are defined by three rotation parameters:  $R_X$ ,  $R_Y$ , and  $R_Z$ , representing the rotations about the x, y, and z-axes, respectively of the image coordinates with respect to the ground control coordinates.

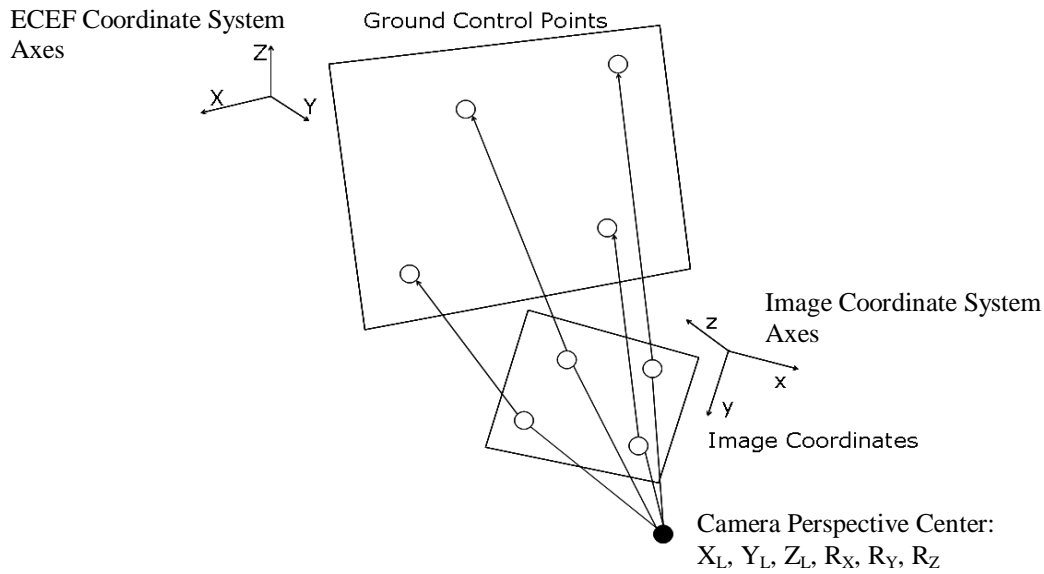


Figure 3.1: Camera Resection. The resection will determine the translational offsets between the geometric lens center and the camera perspective center ( $X_L$ ,  $Y_L$ , and  $Z_L$ ), as well as determine the three rotation parameters  $R_X$ ,  $R_Y$ , and  $R_Z$  to rotate the image coordinate system axes to the Earth Centered Earth Fixed (ECEF) coordinate axes. The resection involves ground control points whose absolute positions are known in the ECEF system, as well as their corresponding image points, and applies the collinearity equations based on these points to determine the six camera parameters listed above.

The position of the rivets on the outside wall of the CAR facility served as the ground control points for the resection. The GPSVan made multiple passes of this wall, so that each camera would be able to image the wall from different distances and orientations. Four of these images were then chosen for each camera, each of which for a different position and orientation with respect to the wall. The images were deliberately

chosen in such a manner to avoid biasing the results by using a single orientation and distance with respect to the wall and ensuring that exterior orientation parameters for the cameras are, indeed, correct. Figure 3.2 shows the differences in position and orientation of the four images chosen for the front left stereo camera. A minimum of eight of the visible ground control points were then selected from each image. These points were dispersed throughout the images and were chosen, so that as many of the same ground control points as possible would be visible between the four different images of each camera. Additionally, these points were selected, so that no three points would be collinear, as collinear points can be expressed as a linear combination of the other points laying on the same line and the use of multiple collinear points is equivalent to using any two points defining that line. The image coordinates of the selected ground control points in pixels, and the three-dimensional positions of the corresponding ground control points were then used as inputs to the collinearity equations to determine the exterior orientation parameters.

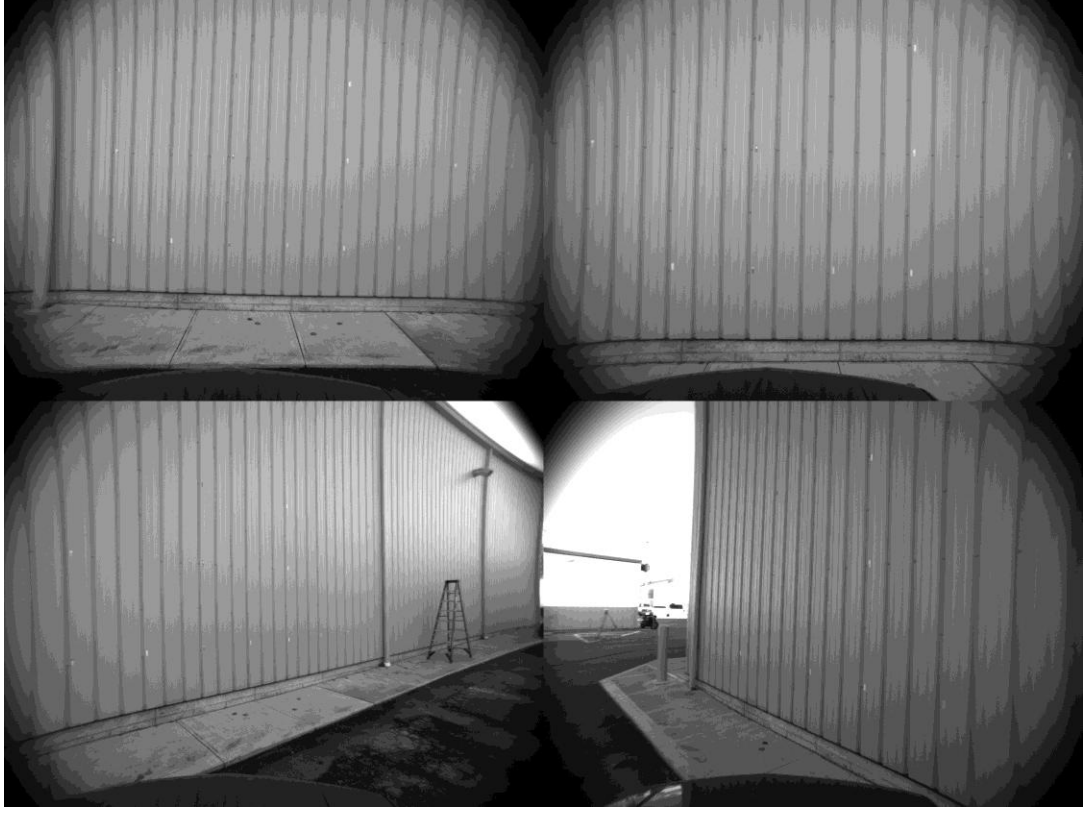


Figure 3.2: Left Front Stereo Camera Images. These are the four images chosen for the resection of the left front stereo camera, sensor 2 in Figure 2.3. Each of these images was taken from the same portion of the wall at different angles and distances from the wall to provide different perspectives.

The collinearity equations are of the form:

$$F_1 = x_i - x_0 + f \times \frac{M_{1,1} \times (X - X_L) + M_{1,2} \times (Y - Y_L) + M_{1,3} \times (Z - Z_L)}{M_{3,1} \times (X - X_L) + M_{3,2} \times (Y - Y_L) + M_{3,3} \times (Z - Z_L)} \quad (3.16)$$

$$F_2 = y_i - y_0 + f \times \frac{M_{2,1} \times (X - X_L) + M_{2,2} \times (Y - Y_L) + M_{2,3} \times (Z - Z_L)}{M_{3,1} \times (X - X_L) + M_{3,2} \times (Y - Y_L) + M_{3,3} \times (Z - Z_L)} \quad (3.17)$$

Where

$F_1$  and  $F_2$  are the observed x and y image coordinates.

$x_i$  and  $y_i$  are the x and y image coordinates (in pixels) of a ground control point.

$x_0$  and  $y_0$  are the x and y coordinates of the principal point in the photo coordinate system and are part of the interior orientation parameters determined independently of this research.

$f$  is the camera focal length, and is one of the interior orientation parameters determined independently of this research.

$X$ ,  $Y$ , and  $Z$  are the coordinates of the ground control point in the Earth Centered Earth Fixed (ECEF) frame corresponding to image point  $(x_i, y_i)$ .

$X_L$ ,  $Y_L$ , and  $Z_L$  are the three-dimensional coordinates of the camera perspective center in the ECEF frame.

$M_{i,j}$  is the corresponding row (i) and column (j) element of the rotation matrix  $M$  calculated as:

$$M = M_Z \times M_Y \times M_X \quad (3.18)$$

Where  $M$  is the overall rotation matrix and  $M_Z$ ,  $M_Y$ , and  $M_X$  are the rotation matrices about the z, y, and x axes respectively, or the heading ( $\kappa$ ), pitch ( $\phi$ ), and roll ( $\omega$ ).

For the cameras:

Rotation about the x-axis is given as:

$$M_X = R_\omega = \begin{bmatrix} 1 & 0 & 0 \\ 0 & \cos \omega & -\sin \omega \\ 0 & \sin \omega & \cos \omega \end{bmatrix} \quad (3.19)$$

Rotation about the y-axis is given as:



$$M_Y = R_\varphi = \begin{bmatrix} \cos \varphi & 0 & \sin \varphi \\ 0 & 1 & 0 \\ -\sin \varphi & 0 & \cos \varphi \end{bmatrix} \quad (3.20)$$

Rotation about the z-axis is given as:

$$M_Z = R_\kappa = \begin{bmatrix} \cos \kappa & -\sin \kappa & 0 \\ \sin \kappa & \cos \kappa & 0 \\ 0 & 0 & 1 \end{bmatrix} \quad (3.21)$$

And the M maxtrix is calculated as:

$$M = R_K \times R_\varphi \times R_W \quad (3.22)$$

and can be expanded to:

$$\begin{bmatrix} \cos \varphi \cos \kappa & \cos \kappa \sin \omega \sin \varphi - \cos \omega \sin \kappa & \sin \omega \sin \kappa + \cos \omega \cos \kappa \sin \varphi \\ \cos \varphi \sin \kappa & \cos \omega \cos \kappa + \sin \omega \sin \varphi \sin \kappa & \cos \omega \sin \varphi \sin \kappa - \cos \kappa \sin \omega \\ -\sin \varphi & \cos \varphi \sin \omega & \cos \omega \cos \varphi \end{bmatrix} \quad (3.23)$$

The collinearity equations require a minimum selection of three non-collinear corresponding image and ground control points. Since more than three points were selected in each image the more rigourous statistical approach of a least squares adjustment was applied using the collinearity equations. A standard Gauss Markov model was applied in the least squares adjustment.

The Gauss Markov least squares model is given as:

$$Ax = f + v \quad (3.24)$$

Where

A is the Jacobian matrix of size 2n x 6 constructed from the partial derivites of the collinearity equation with respect to the unknow parameters (vector x), where n in the number of control points.

$x$  is a 6 x 1 column vector of unknown parameters, whose elements represent the orientation and position of the camera in the order of  $\omega$ ,  $\phi$ ,  $\kappa$ ,  $X_L$ ,  $Y_L$ , and  $Z_L$  (more precisely, they are increments to the approximated parameters (or error states), as the system of observation equations is non-linear, and can be linearized using the approximated parameter vector).

$f$  is a 2n x 1 column vector constructed from the non-linearized collinearity equation.

$v$  is 2n x 1 column vector corresponding to the residuals, or error, of each element in the  $f$  vector.

In the explanation of the equation above, the total number of points selected in an image is represented by  $n$ . Additionally, each point provides two equations (see the collinearity equations 3.16 and 3.17), one for the  $x$  and one for the  $y$  image coordinate. This is why the  $A$  matrix and the  $f$  vector each have a number of rows equal to  $2n$ .

Once the Jacobian matrix ( $A$ ) and the observation vector ( $f$ ) are populated for every point, equation 3.24 can then be solved for vector  $x$  as follows:

$$x = (A^T \times A)^{-1} \times A^T \times f \quad (3.25)$$

Where  $A^T$  denotes the transpose of matrix  $A$  and  $(A^T \times A)^{-1}$  denotes the inverse of the normal matrix resulting from the transpose of the  $A$  matrix multiplied with the original  $A$  matrix.

Since the collinearity equations are nonlinear equations, which were linearized, the vector  $x$  obtained from equation 3.25 does not represent the exact solution of the exterior orientation parameters. Instead, the vector  $x$  calculates increments to each of the

six exterior orientation parameters. Consequently, the above procedures must be repeated until all of the exterior orientation parameters satisfy a condition of convergence. It was assumed for a given iteration if the increment to each of the three translational parameters is less than a tenth of a millimeter and if the increment to each of the rotational parameters is less than a hundredth of a second, then the solution has converged. In the event that the solution has not converged, the updated exterior orientation parameters will be used in the next iteration and if the solution has converged, the updated exterior orientation parameters will be returned as the final exterior orientation parameters. At this point the six exterior orientation parameters are known for the image. This process was then repeated for every image from each camera and the results were recorded.

### *3.2.4 Computation of INS and Camera Lever Arms*

The lever arms between the INS and camera perspective centers can be computed just as the lever arms between the INS and GPS and between the INS and camera lens center – using the coordinates of both points known now in the same coordinate frame. Since the relationship between the GPS and INS is known along with the GPS time at which the images were acquired, it is possible to determine the position of the center of the INS at the time when the images were acquired. With the results of the resection the coordinates of the camera perspective center are also known at the time of exposure. Therefore, it is now possible to calculate the three translational offsets between the INS and the perspective center of each camera. Since there were multiple images for each camera, the lever arm is computed for each image and the average of the lever arms from

the four selected images of a given camera will be used as the true lever arm between the INS and that particular camera.

### 3.2.5 Determination of the Boresight Matrix

Now that the orientation of the camera perspective centers are known from the resections performed in chapter 3.2.4, the three rotational offsets between the INS and each camera can be calculated in accordance with the method established by Wegmann [Wegmann, 2002]. This will also consider the case of a single camera, as an identical process will be applied to the remaining cameras. The rotations about the X, Y, and Z axes relating the axes of the INS and image coordinate system of each camera to the ECEF coordinate system are known from the resection. Therefore, it is possible to determine the three rotations relating the image coordinate system of a given camera to the INS axes. It is also assumed that all rotations will be done in the counter-clockwise direction in the following order for both the INS and camera: heading, pitch, then roll. The individual rotation matrices for the INS and camera are constructed according to equations 3.19, 3.20, and 3.21. Next, the INS and camera-derived attitude matrices are computed as:

$$\mathbf{M}_{INS} = \mathbf{R}\omega_{INS}\mathbf{R}\phi_{INS}\mathbf{R}\kappa_{INS} \quad (3.26)$$

$$\mathbf{M}_{CAM} = \mathbf{R}\omega_{CAM}\mathbf{R}\phi_{CAM}\mathbf{R}\kappa_{CAM} \quad (3.37)$$

Where  $\mathbf{M}_{INS}$  is the INS-derived attitude matrix and  $\mathbf{M}_{CAM}$  is the camera-derived attitude matrix.

The boresight rotation matrix can then be calculated as:

$$\mathbf{R}_b = \mathbf{M}_{INS}^T \mathbf{M}_{CAM} \quad (3.28)$$

Equation 3.28 can be expanded to:

$$R_b = \begin{bmatrix} \cos \varphi \cos \kappa & -\cos \varphi \sin \kappa & \sin \varphi \\ \cos \omega \sin \kappa + \sin \omega \sin \varphi \cos \kappa & \cos \omega \cos \kappa - \sin \omega \sin \varphi \sin \kappa & -\sin \omega \cos \varphi \\ \sin \omega \sin \kappa - \cos \omega \sin \varphi \cos \kappa & \sin \omega \cos \kappa + \cos \omega \sin \varphi \sin \kappa & \cos \omega \cos \varphi \end{bmatrix} \quad (3.29)$$

Equation 3.29 can be represented in the following form:

$$R_b = \begin{bmatrix} r_{11} & r_{12} & r_{13} \\ r_{21} & r_{22} & r_{23} \\ r_{31} & r_{32} & r_{33} \end{bmatrix} \quad (3.30)$$

The boresight rotation angles are then extracted as:

$$d\varphi = \sin^{-1}(r_{13}) \quad (3.31)$$

$$d\omega = \tan^{-1}(-r_{23}/r_{33}) \quad (3.32)$$

$$d\kappa = \tan^{-1}(-r_{12}/r_{11}) \quad (3.33)$$

Where

$d\varphi$  is the boresight pitch

$d\omega$  is the boresight roll

$d\kappa$  is the boresight heading

Similar to the camera lever arms, this process will determine the rotational offsets for each of the four images used by each camera. The average of the each of the four pitch, roll, and heading angles will be used to derive the overall boresight pitch, roll, and heading angles for a camera. This process is then repeated for every camera. The results of the resection are shown in Table 3.1.

### 3.3 Relative Orientation

#### *3.3.1 Introduction*

Relative orientation is the process of determining the translational and rotational offsets between stereo cameras. This information is needed when setting up a stereo model from the cameras, so that it is possible to recover three-dimensional information from the scene. The stereo model is made possible only in the overlapping field of views of the stereo cameras. Each camera observes features in the overlapping scene from a different perspective, allowing the use of photogrammetric techniques to back project light rays from the matching image points and recreate the three-dimensional scene based on the interception of these rays. In order for this process to work, however, the exterior orientation parameters for both cameras must already be known.

Traditionally, the relative orientation is done because the full exterior orientation parameters of both cameras are not known. Since there are two cameras involved and each camera has a total of six exterior orientation parameters, there are a total of twelve parameters that must be solved for. However, seven of these parameters can be fixed, reducing the number of unknown parameters to five. There are two distinct cases of relative orientation depending on which five exterior orientation parameters between the two cameras are the unknowns: dependent and independent relative orientation. In dependent relative orientation, all of the exterior orientation parameters for one camera are known as well as one of the translational components between the cameras. While this known translational component or baseline does not fix the other camera in space, it restricts its possible translations to two axes as well as three possible rotations. In

independent relative orientation the translational components of both cameras are known and the rotational components are unknown. One of the rotational components for one of the cameras is then fixed, allowing for the other rotational components of both cameras to be solved. In both cases, the remaining five parameters can be solved for by selecting a minimum of five intervisible points between images from both cameras and inputting the pixel coordinates of these points into a least squares adjustment. In the case of independent relative orientation the adjustment will use the collinearity equations and will also require the coordinates of matching ground control points. In the case of dependent relative orientation the coplanarity equation will be used in the least squares adjustment and ground control points will not be required due to different geometry of the coplanarity equations. The process of dependent relative orientation is illustrated in Figure 3.3.

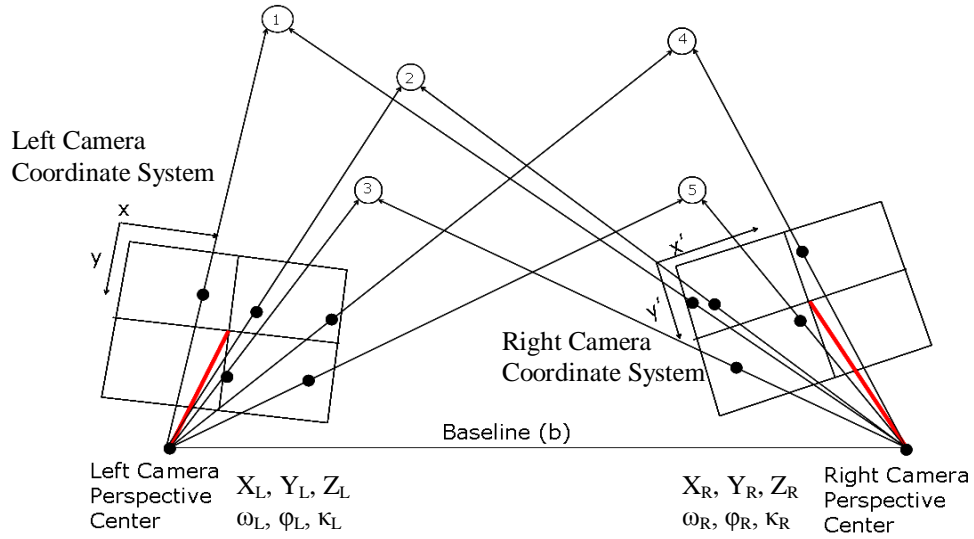


Figure 3.3: Dependent Relative Orientation Geometry. The red lines from the perspective center of each camera to the photographs represent the feet of the perspective centers dropped perpendicular to the photograph and show the location of the principal points. All parameters defining the exterior orientation of the left image are known and only the Y coordinates, provided by the baseline between camera perspective centers, is known for the right camera. This leaves the  $X_R$  and  $Z_R$  coordinates as well as the roll ( $\omega_R$ ), pitch ( $\phi_R$ ), and heading ( $\kappa_R$ ) angles to be solved for. These parameters are solved for by selecting at least five linearly independent points visible in both images (points 1 through 5 in the figure) and applying the collinearity equations to determine the unknown parameters.

### 3.3.2 Computing Relative Orientation

The case at hand fits neither dependent or independent relative orientation, as all exterior orientation parameters for the cameras were determined during resection. However, generation of a stereo model still requires that the translational and rotational offsets between cameras be computed. Since the boresight transformation has been determined, the exterior orientation parameters of both cameras are known with certainty at the time of image acquisition. Furthermore, after disregarding very minor manufacturing errors and the possibility of minute differences in the delay between the



time when the camera takes the image and when the image is actually acquired, each camera can be regarded as having the same imaging rate. This results in both stereo cameras acquiring images at the same time, and at that GPS time, the exterior orientation of both cameras are known from GPS/INS and the boresight transformation that together fix them in space. This makes it possible to compute the translational and rotational offsets between the two cameras in the same way the boresight offsets were determined. For convention, the offsets will define the translation vectors and rotation matrix from the left camera to the right camera for both the front and back sets of stereo cameras. The results of the relative orientation are shown in Table 3.2.

Sensor	Description	Front (m)	Right (m)	Up (m)	$R_x$	$R_y$	$R_z$	std $R_x$	std $R_y$	std $R_z$
1	INS to Left Side	326471.8624	4429597.998	196.359375	89.56656	0.419452	270.9703	0.313257	0.038739	1.165534
2	INS to Front Left	326471.4469	4429593.682	196.209	88.86662	0.183443	-0.45992	0.31654	0.096313	0.823289
3	INS to Front Right	326471.4205	4429594.265	196.240278	88.19852	0.425331	-0.68597	0.462389	0.104532	1.769497
4	INS to Right Side	326471.4064	4429594.935	196.220167	89.57877	-0.64209	90.50115	0.75737	0.178545	3.319669
5	INS to Back Right	326471.4948	4429594.909	196.19475	90.34189	-0.18009	179.9956	0.276313	0.143466	0.831953
6	INS to Back Left	326471.3705	4429596.659	196.304737	89.53806	-0.20635	178.5698	0.199141	0.295346	0.507036

Table 3.1: Resection Results. This table displays the six parameters determined through the resection for each camera, as well as the standard deviation of the three orientation parameters.

69

Sensors	Description	Front (m)	Right (m)	Up (m)	$\omega$	$\phi$	$\kappa$
2 to 3	Front Left to Front Right	-0.02641684	0.583	0.03127759	-0.66111	-0.88777	0.861429
6 to 5	Back Left to Back Right	-0.12430247	1.75	0.10998739	0.804152	-1.60855	0.224813

Table 3.2: Relative Orientation Results. Table 3.2 shows the results of the relative orientation between the front left and back left stereo cameras, listing the three translational and three rotational parameters. These parameters define the relationships from sensor 2 to sensor 3 and sensor 6 to sensor 5.

## Chapter 4 Conclusions and Future Work

The determination of multi-sensor inter-relationships is a delicate task requiring the utmost detail in precision and accuracy. Accuracy, in particular, is extremely important, as all subsequent steps build on the results of the first step, the survey. It is therefore of the utmost importance to ensure that the survey is done with the highest possible accuracy, as any errors in the positions of sensors or ground control points determined during the survey will propagate to subsequent steps and result in the determination of incorrect relationships between sensors. Ramifications of this include the incorrect geo-spatial registration of imagery, resulting in the extraction of incorrect geo-spatial information from them, and the extraction of incorrect navigation information if image-to-image matching is used for navigation. If the errors in the sensor inter-relationship are small than the image data may still be suited for mapping purposes as long as the results do not exceed the accuracy standards of the mapping project. If the accuracy fails to meet these standards the sensor inter-relationships must be re-determined, beginning once more with the survey.

Errors in the survey impacting accuracy can be reduced in several ways. The first among them is ensuring that the precision setting on the total station is set to the desired level of measurements. Precision itself refers to the degree with which

measurements are repeatable and if the total station's precision setting is greater than the user's desired precision level then the survey results are not going to be very precise. This will impact the accuracy, as the total station will not be able to take readings to the desired position of a sensor or control point. To mitigate these effects the precision of distances was set to a millimeter and the precision of angular measurements was set to a tenth of a degree. Other sources of error were removed from the survey through following good surveying practices and by planning out the survey prior to beginning. The later step allowed for a site reconnaissance prior to the survey to better formulate the methods to be used and for multiple and independent reviews of the survey plan prior to beginning, with built in time to revise the plan in the event that any major problems detected. Also, checks were done during the survey to ensure that good surveying practices were being used to mitigate the introduction of blunders during the survey. With the proper precision and checking standards in place, the only errors entering into the survey were random errors, which are small errors intrinsic to the measurement process and cannot be avoided.

The other major source of errors entering into the measurement process is the camera resection. Errors could enter this step during the selection of ground control points in each image. All measurements of the rivets on the exterior wall were performed to the center of the rivet. Therefore, the best results are only obtainable if the center of a rivet is visible when recording the pixel coordinates of that point. Furthermore, the best measurements can only be made if the rivet is fully visible in the image, which requires more than a small portion protruding from a wall to be seen. A final consideration with

selecting control points relates to the pixel size, as this will determine the smallest discernable measurement in the image. The pixel size in all images is small enough to represent all rivets as multiple pixels but the center of the rivet may not necessarily be the center pixel representing the object. Furthermore, the method used to measure the pixel coordinates of a selected point was based on the upper left corner of the pixel and was able to determine pixel position on a sub-pixel level with a precision to the hundredths place. This precision made possible a more accurate determination of the rivet centers and helped to ensure a high accuracy standard for determining the inter-relationships between the cameras and INS.

Determining the inter-relationships among the sensors was the scope of this thesis and now that these relationships have been determined they will be applied to support mapping and navigation from the GPSVan. Mapping can be done using the exterior orientation parameters and relative orientation for both sets of stereo cameras to determine the intersection of matching image points in space and generate georeferenced three-dimensional models. More immediate work will be done with the calibration results in image-to-image navigation. Here, matching of features from successive images for each camera will be used to determine the changes in attitude of the GPSVan. This information will be combined with the change in odometer readings between successive images as an alternative method of determining the attitude and position of the GPSVan in areas of GPS obstructions.

## References

- [Grejner-Brzezinska, 2001a] Grejner-Brzezinska, D. A. (2001a). "Mobile Mapping Technology: Ten Years Later Part I". *Surveying and Land Information Systems*, 61(2):79-94.
- [Grejner-Brzezinska and Toth, 2000] Grejner-Brzezinska, D. A. and Toth, C. K. (2000). "Precision Mapping of Highway Linear Feature". *International Archives of Photogrammetry and Remote Sensing*, XXXIII-B2:233-240.
- [Grejner-Brzezinska, 2011] Grejner-Brzezinska, D. A. "Introduction to GPS Theory and Applications." GS 608 Lecture. The Ohio State University. April 2011.
- [Grejner-Brzezinska, 2012] Grejner-Brzezinska, D.A.(2012). "Mobile Mapping Systems: what they are and why are they becoming a mapping standard?" Summer School on Mobile Mapping Technology, Tainan, Taiwan, June 11-15, 2012.
- [Ho, 2009] Ho, M. "Geoid." Geodetic Glossary. Sep. 2001. National Geodetic Survey. 18, Jan. 2012. <[http://www.ngs.noaa.gov/CORS-Proxy/Glossary/xml/NGS\\_Glossary.xml](http://www.ngs.noaa.gov/CORS-Proxy/Glossary/xml/NGS_Glossary.xml)>.
- [Jekeli, 2001] Jekeli Ch. (2001). "Inertial Navigation Systems with Geodetic applications". Walter de Gruyter Berlin, New York.
- [Ramirez, 2010] Ramirez, R. (2010). "GS 563 Lecture Notes." GS 208 Lecture. The Ohio State University. November 2010.

- [Skaloud et al., 1996] Skaloud, J., Cramer, M., and Schwarz, K. (1996). "Exterior orientation by direct measurement of camera position and orientation". Pages 125-130.
- [Wegmann, 2002] Wegmann, H. (2002). "Image Orientation by Combined (A)AT with GPS and IMU." Volume 34, pages 279-284. ISPRS Commission I/Pecora, Denver, USA.
- [Wooden, 1985] Wooden, W.H., (1985). "Navstar Global Positioning System, Proceedings of the First International Symposium on Precise Positioning System", Rockville, Maryland, April 15-19, Vol. 1, pp. 23-32.